

# Early Holocene ice retreat from Isle Royale in the Laurentian Great Lakes constrained with $^{10}\text{Be}$ exposure-age dating

Eric W. Portenga<sup>1</sup>, David J. Ullman<sup>2</sup>, Lee B. Corbett<sup>3</sup>, Paul R. Bierman<sup>3</sup>, Marc W. Caffee<sup>4</sup>

<sup>1</sup> Geography and Geology Department, Eastern Michigan University, Ypsilanti, MI 48197, USA

5 <sup>2</sup> Geology Department, Northland College, Ashland, WI 54806, USA

<sup>3</sup> Rubenstein School of Natural Resources and the Environment, University of Vermont, Burlington, VT 05405, USA

<sup>4</sup> Department of Physics and Astronomy and Department of Earth, Atmospheric, and Planetary Sciences, Purdue University, West Lafayette, IN 47907, USA

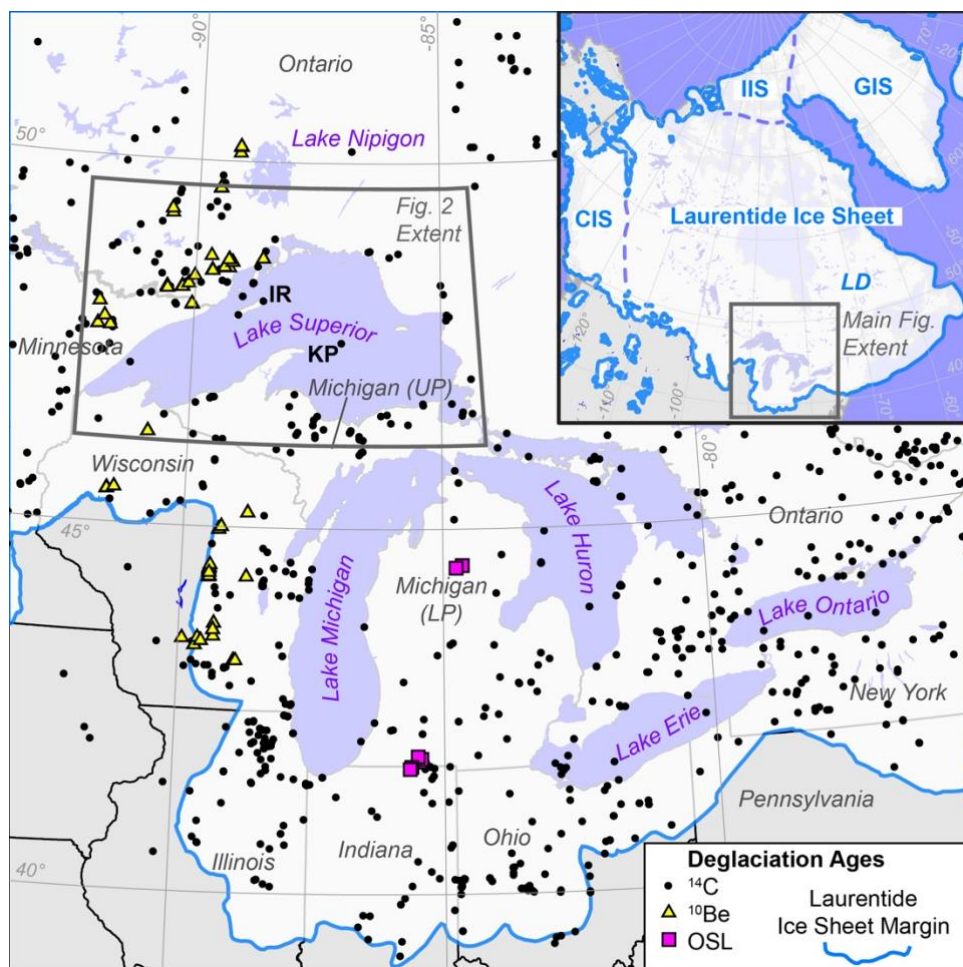
*Correspondence to:* Eric W. Portenga (eric.portenga@emich.edu)

10 **Abstract.** The timing of the Laurentide Ice Sheet's final retreat from North America's Laurentian Great Lakes is relevant to understanding regional meltwater routing, changing proglacial lake levels, and lake-bottom stratigraphy following the Last Glacial Maximum. Recessional moraines on Isle Royale, the largest island in Lake Superior, have been mapped but not directly dated. Here, we use the mean of ten new  $^{10}\text{Be}$  exposure-ages of glacial erratics from two recessional moraines ( $10.1 \pm 1.1$  ka, one standard deviation; excluding one anomalously young sample) to constrain the timing of Isle Royale's final  
15 deglaciation. This  $^{10}\text{Be}$  age is consistent with existing minimum limiting  $^{14}\text{C}$  ages of basal organic sediment from two inland lakes on Isle Royale, a sediment core in Lake Superior southwest of the island, and an estimated deglaciation age of the younger of two subaqueous moraines between Isle Royale and Michigan's Keweenaw Peninsula. Relationships between Isle Royale's landform ages and Lake Superior bottom stratigraphy allow us to delineate the retreat of the Laurentide ice margin across and through Lake Superior in the early Holocene. We suggest Laurentide ice was in contact with the southern  
20 shorelines of Lake Superior later than previously thought.

## 1 Introduction

Following the Last Glacial Maximum (LGM), the southwest margins of the Labrador Dome of the Laurentide Ice Sheet (LIS) retreated, exposing the Laurentian Great Lakes of North America (hereafter referred to as the Great Lakes, Fig. 1). Initial retreat of the LIS from LGM margins in the Great Lakes region is associated with increased summer boreal insolation  
25 (Clark et al., 2009; Ullman et al., 2015), and much of meltwater from the melting LIS drained through the Great Lakes throughout the late Pleistocene and early Holocene (Carlson et al., 2007; Fisher, 2020; Teller and Thorleifson, 1983; Teller et al., 1983). Overall, meltwater from the LIS accounts for ~50–60% of the late-Pleistocene sea-level budget (Clark and Mix, 2002). Constraining spatial and temporal retreat patterns of the LIS retreat, including along its southern margins through the Great Lakes, improves our understanding of meltwater routing from proglacial lakes to the oceans and proglacial lake

30 organization (Breckenridge, 2013; Broecker, 2006; Broecker et al., 1989; Carlson et al., 2007; Farrand, 1969; Fisher, 2020; Fisher and Breckenridge, 2022; Leydet et al., 2018; Teller, 1990; Teller and Mahnic, 1988; Teller et al., 2002, 2005).



35 **Figure 1.** The Laurentian Great Lakes of North America and the Laurentide Ice Sheet (LIS) margins at the Last Glacial Maximum (LGM; solid blue line; Ehlers et al., 2011). Inset figure shows full extent of the North American LGM ice cover inclusive of the Cordilleran (CIS), Greenland (GIS), Innuitian (IIS) Ice Sheets (Ehlers et al., 2011) and the Labrador Dome (LD) where ice that forms the Laurentide Ice Sheet's southern margins originates. Existing sample sites for  $^{14}\text{C}$  data (black dots; Dalton et al., 2020),  $^{10}\text{Be}$  data (yellow triangles; Ceperley et al., 2019; Kelly et al., 2016; Leydet et al., 2018; Lowell et al., 2021; Ullman et al., 2015), and OSL (purple squares; Fisher et al., 2020; Schaetzel et al., 2017). Only US states and Canadian provinces covered by the Laurentide Ice Sheet are shown; the state of Michigan comprises the lower peninsula (LP) and upper peninsula (UP). Locations of Isle Royale (IR) and Keweenaw Peninsula (KP) are shown.

40

Although previous work has investigated the age and rate of ice retreat through the Great Lakes region (Dalton et al., 2020; Dyke, 2004), geochronological constraints on the timing of ice retreat are sparse, especially within lake basins, and Dalton et al. (2020) note that the chronology of Laurentide Ice retreat through the Great Lakes has not received as much attention by researchers as other margins of the LIS over the last twenty years. The existing chronology of ice retreat from the Great

45

Lakes is constrained primarily by minimum-limiting  $^{14}\text{C}$  ages, most of which come from the southern LGM margins of the LIS (Dyke, 2004; Dalton et al., 2020; Fig. 1). Additional constraints on the timing of ice retreat from the Great Lakes region include  $^{10}\text{Be}$  exposure age dating (Ceperley et al., 2019; Colgan et al., 2002; Leydet et al., 2018; Lowell et al., 2021; Ullman et al., 2015; Fig. 1) and in some cases, optically stimulated luminescence burial-age dating (e.g. Fisher et al., 2020; Schaetzl et al., 2017). As a note, all ages in this study with units of cal ka BP are published  $^{14}\text{C}$  calibrated ages and were rounded to the nearest 100 years; none are significantly different than those recalibrated using CALIB rev. 8 (Stuiver et al., 1993).

Lake Superior is the largest and northernmost of the Great Lakes and the largest freshwater lake by surface area in the world (IAGLR, 2012). Despite decades of geochronological efforts mapping ice margin positions across Lake Superior (e.g. Bajc et al., 1997; Black, 1976; Leydet et al., 2018; Lowell et al., 1999, 2005, 2009, 2021; Saarnisto, 1974), the long distances between shorelines and the paucity of dateable organic material retrieved from lake-bottom sediments has hampered development of a detailed history of LIS retreat across the lake (Breckenridge, 2007; Breckenridge et al., 2004; Hyodo and Longstaffe, 2011). Thus, uncertainties about LIS retreat across the lake following the LGM, and hence meltwater routing and proglacial lake organization, remain. Ice retreat through the Great Lakes appears to have been mostly continuous across the late-Pleistocene-Holocene transition (Lowell et al., 2021) with some clear exceptions of moderate ice re-advance during the Younger Dryas stadial (Carlson, 2010; Loope, 2006; Lowell et al., 1999, 2009). The timing of this advance, known as the Marquette Readvance, is well constrained at the Lake Gribben forest bed site in Michigan's upper peninsula (UP) to  $\sim 11.9$  cal ka BP (Fig. 2a; Lowell et al., 1999), and it is known to have produced the Grand Marais I moraine complex across the UP and the Marks moraine in Ontario (Fig. 2; Carlson, 2010; Hobbs and Breckenridge, 2011; Loope, 2006; Lowell et al., 1999, 2009). There is less agreement regarding how far ice advanced in the western Lake Superior basin during the Marquette Readvance (Fig. 2b; Black, 1976; Clayton and Moran, 1982; Colman et al., 2020; Drexler et al., 1983; Farrand and Drexler, 1985; Peterson, 1985). This uncertainty results from little dateable material in Lake Superior sediments, the lack of well-defined ice-marginal deposits associated with the Marquette Readvance around the western Lake Superior basin, and ongoing discussion about how some  $^{14}\text{C}$  ages and the stratigraphy they come from should be interpreted (Colman et al., 2020; Hobbs and Breckenridge, 2011).

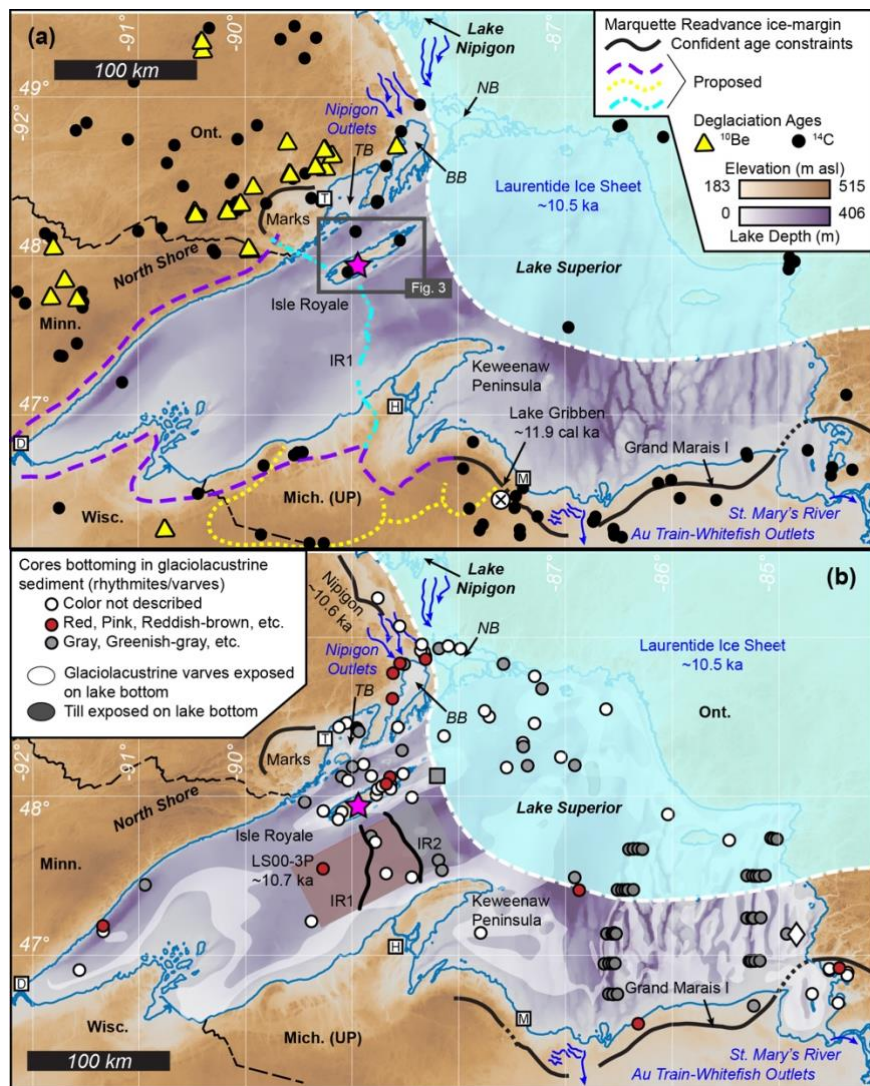
Much of the recent geochronological work around Lake Superior focuses on retreat of the LIS's Superior Lobe along the northwest shore (the North Shore; Fig. 2a) leading up to and following the Marquette Readvance, rather than establishing cross-lake relationships between the North Shore and Wisconsin or Michigan's UP (Fig. 2). For example, near-constant retreat of the Superior Lobe along the Lake Superior North Shore uncovered eastward-draining outlets from glacial Lake Agassiz to the Lake Superior basin via Lake Nipigon (Fig. 2; Fisher, 2020; Kelly et al., 2016; Leydet et al., 2018; Lowell et al., 2009, 2021; Teller and Mahnic, 1988). Organic  $^{14}\text{C}$  and  $^{10}\text{Be}$  exposure ages of landforms along the North Shore constrain deglaciation of these outlets from Lake Nipigon to Lake Superior at Black Bay at  $\sim 10.7$  ka (Fig. 2a; mean of  $^{10}\text{Be}$  ages; Leydet et al., 2018; Lowell et al., 2021; Teller and Mahnic, 1988). Meltwater from proglacial lakes flowed through western

Lake Superior to eastern Lake Superior and drained first to Lake Michigan through the Au Train-Whitefish Outlets across Michigan's UP and later through the St. Mary's River (Fig. 2; Breckenridge, 2013). However, the path meltwater took through Lake Superior during this drainage is unclear because ice margin positions remain less well-constrained since there is less recent research and few numerical deglaciation ages across Michigan's UP and none along the Keweenaw Peninsula (Fig. 2a; Drexler, 1981; Huber, 1973; Hughes, 1963).

In the absence of quantitative dating across much of the Lake Superior region, much of our knowledge of the chronology of LIS retreat here comes from analyses of the Lake Superior lake-bottom stratigraphy, which primarily consists of pre-Marquette Readvance outwash or till, then red glaciolacustrine sediment (i.e. varves; Breckenridge, 2007), gray varves, and lastly post-glacial Holocene sediments (Farrand, 1969). The older red varves are sourced from red clay, till, and/or bedrock in the southwest Lake Superior region, compared to the younger gray varves, which are sourced from the bedrock of the Canadian Shield (Breckenridge et al., 2021; Farrand, 1969). Lake Agassiz drainage into the Lake Superior basin is associated with the onset of red varve deposition in areas that were ice-free at the time (Fig. 2b; Breckenridge and Johnson, 2009), most likely when lake levels were between Duluth and Minong stages (Breckenridge, 2004; Colman et al., 2020; Teller and Mahnic, 1988). In the western Lake Superior basin, red varves are identified north of Isle Royale, in some inland lakes on Isle Royale's northern margin (Figs. 2b, 3a), and down-ice of the IR2 moraine (Fig. 2b; Breckenridge, 2007; Breckenridge et al., 2004; Colman et al., 2020; Maher, 1977; Raymond et al., 1975; Teller and Mahnic, 1988). Red varves are also observed in parts of the eastern Lake Superior basin (Fig. 2b; Breckenridge et al., 2004; Fisher and Whitman, 1999; Mothersill, 1985), indicating the western and eastern parts of the Lake Superior basin were hydrologically linked. Red varves have not been clearly or consistently reported for areas of the northern Lake Superior basin. Varves are ubiquitous in the northern Lake Superior basin, however, but are gray in color, if any color is reported at all, and are usually associated with ice retreat from the lake basin altogether (Fig. 2b; Breckenridge, 2007; Breckenridge et al., 2004; Colman et al., 2020; Dell, 1973, 1976; Farrand, 1969; Halfman and Johnson, 1984; Hyodo and Longstaffe, 2011; Johnson, 1980; Johnson and Fields, 1984; Kemp et al., 1978; Landmesser et al., 1982; Maher, 1977; Mothersill, 1979, 1985, 1988; Mothersill and Fung, 1972; O'Beirne, 2013; Raymond et al., 1975; Teller and Mahnic, 1988; Thomas and Dell, 1978; Yu et al., 2010). Where red varves are absent in Lake Superior, gray varves directly overlie pre-Marquette Readvance till or outwash, including at a shallow rise just northeast of Isle Royale (gray square in Fig. 2b; Mothershill and Fung, 1982).

Isle Royale is the largest island in Lake Superior (Fig. 2), and it is proximal to and strikes parallel with the well-constrained North Shore deglaciation chronology (Fig. 2; Kelly et al., 2016; Leydet et al., 2018; Lowell et al., 2009, 2021). Isle Royale's position within Lake Superior offers the opportunity to extend the limits of the existing deglacial chronology and draw chronological relationships between the north and south shores of the Lake Superior basin and the lake bottom stratigraphy therein. In this study, we present eleven new  $^{10}\text{Be}$  exposure ages of glacial erratics from the crests of recessional moraines on Isle Royale (Huber, 1973), which are broadly constrained by one existing  $^{14}\text{C}$  age from each of two inland lakes on Isle

115 Royale northeast and southwest of these moraines (Flakne, 2003). We place our interpretation of this new  $^{10}\text{Be}$  exposure-age dataset in the context of the existing Lake Superior deglaciation chronology, various Lake Superior bottom stratigraphy records, relationships drawn between regional subaerial and subaqueous glacial landforms, and the organization of proglacial lakes that occupied the western Lake Superior basin following the Marquette Readvance.



120 **Figure 2.** Maps showing the Lake Superior region of North America and the position of the Laurentide Ice Sheet at ~10.5 ka (Breckenridge, 2007), location of new  $^{10}\text{Be}$  data presented in this study (pink star). Abbreviated locations of the Lake  
 125 Superior basin mentioned in this study include Thunder Bay (TB), Black Bay (BB), and Nipigon Bay (NB); regional cities include Duluth (D), Houghton (H), Marquette (M), and Thunder Bay (T). Background imagery is 3 arcsecond Bathymetry of Lake Superior dataset, which shows elevations in meters above sea level and depths below present-day lake level (NOAA Great Lakes Environmental Research Lab, 1999). A. The Lake Superior basin is shown with locations of moraines known to be associated with the Marquette Readvance (solid black lines). Moraine names are shown with unformatted black text (Isle Royale Moraines 1 and 2: IR1, IR2, respectively; Colman et al., 2020), and ice margin positions thought to be associated with the maximum extent of ice during the Marquette Readvance are shown: dashed purple line (Black, 1976; Clayton and

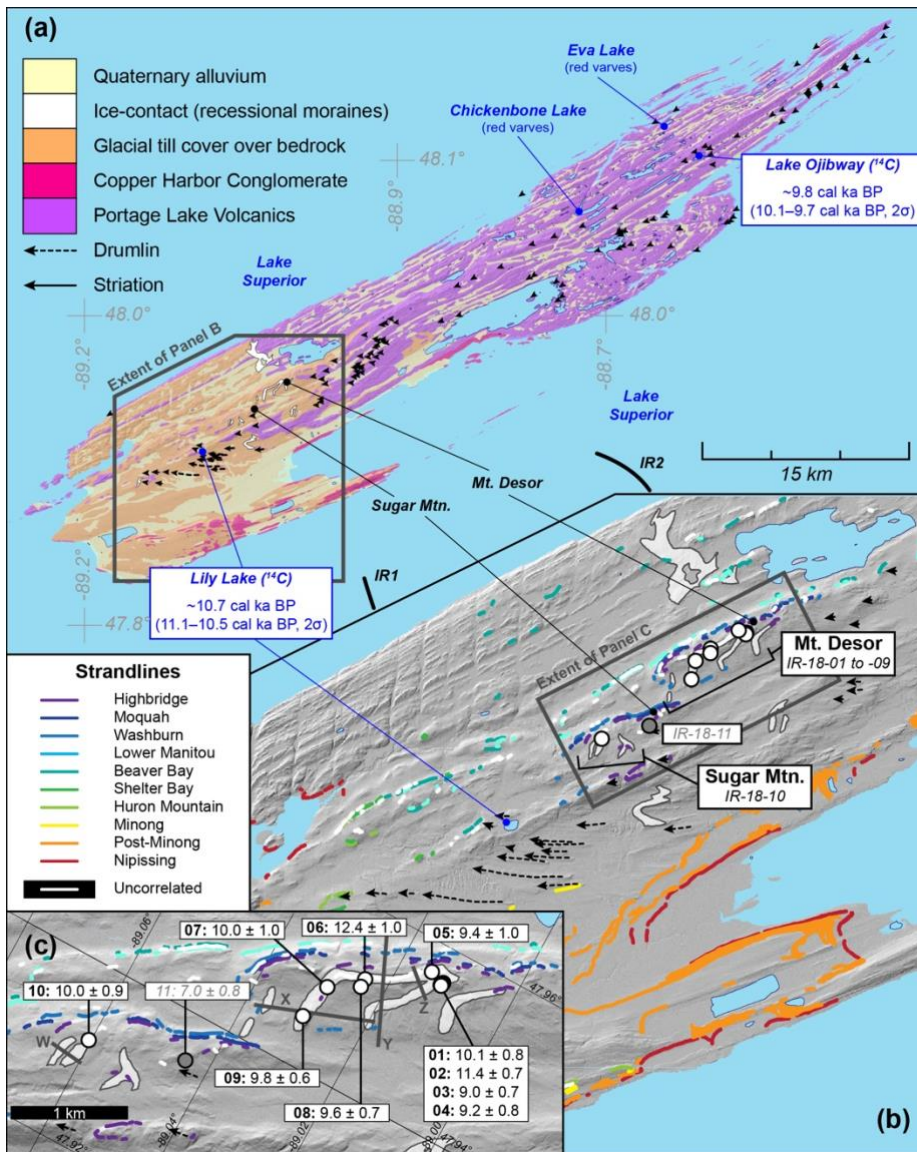
130 Moran, 1982; Drexler et al., 1983; Hughes and Merry, 1978); stippled yellow line (Peterson, 1985); cyan dash-dot line  
(Colman et al., 2020). Black dots and yellow triangles show existing  $^{14}\text{C}$  and  $^{10}\text{Be}$  data locations, respectively (Dalton et al.,  
2020; Leydet et al., 2018; Lowell et al., 2021; Ullman et al., 2015). The Lake Gribben forest bed site is specifically shown  
by a white circle with a black X (Lowell et al., 1999). B. The Lake Superior basin is shown with locations of cores where  
135 varves (red, gray, or no color reported) have been identified and the LS00-3P sediment core (Breckenridge, 2007). The gray  
square northeast of Isle Royale is a shallow rise where gray varves sit directly over pre-Marquette Readvance till (Mothersill  
and Fung, 1972). Red and gray shaded areas south of Isle Royale show extend of red and gray varve deposition, relative to  
the IR1 and IR2 moraines (Colman et al., 2020).

## 2 Study Location: Isle Royale and the Lake Superior Basin

The landscape of Isle Royale is characterized by glacial sediments that blanket the ~1.1 Ga Portage Lake Volcanics and Copper  
Harbor Conglomerate on the southwest third of the island (Fig. 3a; Davis et al., 2022; Elling et al., 2022; Huber, 1973). Glacial  
140 striae are oriented parallel to bedrock ridges and indicate northeast-to-southwest Laurentide Ice flow where bedrock is exposed,  
but striae and craig-and-tail structures (mapped as drumlins) indicate east-to-west ice flow where bedrock is covered by glacial  
till. Striae and craig-and-tail structures point to and terminate at arcuate ice marginal deposits that mark recessional positions  
of Laurentide Ice following the Marquette Readvance (Fig. 3; Huber, 1973).

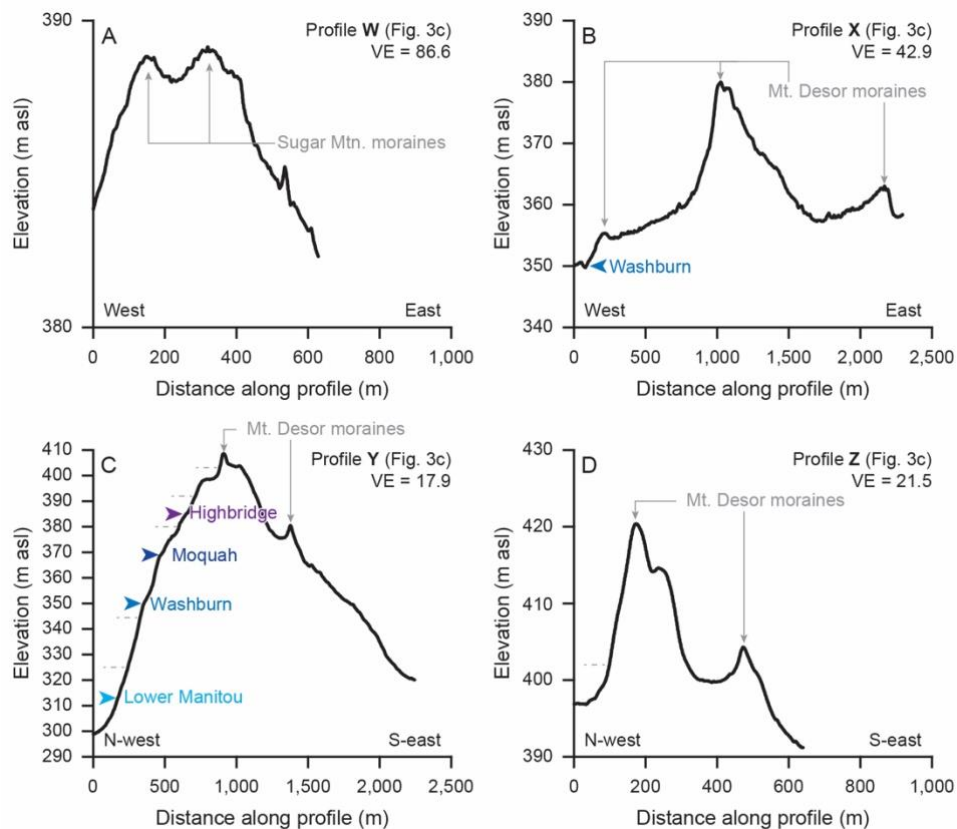
145 The topographical expression of ice-marginal landforms (Fig. 4) is an indication they are recessional moraines that were  
formed subaerially and not reworked by wave processes (Huber, 1973). These moraines have never been directly dated, but  
they are bounded by minimum-limiting  $^{14}\text{C}$  ages on bulk organic sediments extracted from the bottoms of cores at Lily Lake  
and Lake Ojibway on Isle Royale's southwest and northeast ends, respectively (Fig. 3A; Flakne, 2003), which record ice-free  
conditions on Isle Royale by ~10.7 cal ka BP (Lily Lake; median age;  $2\sigma$  age range of 11.1–10.5 cal ka BP) and ice retreat  
150 from Isle Royale by ~9.8 cal ka BP (Lake Ojibway; median age;  $2\sigma$  age range of 10.1–9.7 cal ka BP). Paleomagnetic  
reconstructions and varve counting for a sediment core southwest of Isle Royale (LS00-3P; Fig. 2b), indicate this site was ice  
free by at least ~10.7 ka (Fig. 2; Breckenridge, 2007). Dated strandlines that were correlated across the western Lake Superior  
basin, including Isle Royale, constrain the drawdown of glacial Lake Duluth to post-Minong levels to a two-century period  
between ~10.8–10.6 cal ka BP, draining first to the Lake Michigan basin via the Au Train-Whitefish outlets and ultimately to  
155 the St. Mary's River (Figs. 2, 3b; median ages as presented in Breckenridge, 2013).

Two prominent subaqueous moraines (IR1 and IR2) span the western Lake Superior basin from Isle Royale to Michigan's  
Keweenaw Peninsula but have never been associated with any land-based moraines nor have they been dated directly (Figs.  
2, 3; Breckenridge, 2013; Colman et al., 2020; Landmesser et al., 1982). Formation of the IR2 moraine is estimated at ~10.5–  
160 10.2 ka (Colman et al., 2020), based on the presence of red varves found only on the down-ice side of IR2, the transition from  
red to gray varves at the LS00-3P core (Fig. 2; Breckenridge, 2007), and correlations to the dated red-to-gray varve transition  
in cores from the eastern Lake Superior basin (Breckenridge et al., 2004; Hyodo and Longstaffe, 2011).



165 **Figure 3.** A. Bedrock and surficial geological map of Isle Royale (NPS, 2008), locations of subaqueous moraines IR1 and  
 IR2 (Colman et al., 2020) and inland lakes (Flakne, 2003; Raymond et al., 1975).  $^{14}\text{C}$  ages are median ages of the  $2\sigma$   
 calibrated age range. B. Isle Royale's recessional moraines (Huber, 1973) and named strandlines (Breckenridge, 2013).  
 170 Locations of samples from this study are shown by circles; IR-18-11 is shaded gray because it is anomalously younger than  
 other samples and not included in the mean age of deglaciation we present for Isle Royale. C. Locations of samples relative  
 to positions of Isle Royale's highest moraines and strandlines (see Figures 4, 5). Bold numbers are sample IDs following the  
 format IR-18-XX. Solid gray lines (W-Z) are topographic profiles in Figure 4. LiDAR imagery courtesy of Isle Royale  
 National Park.

175



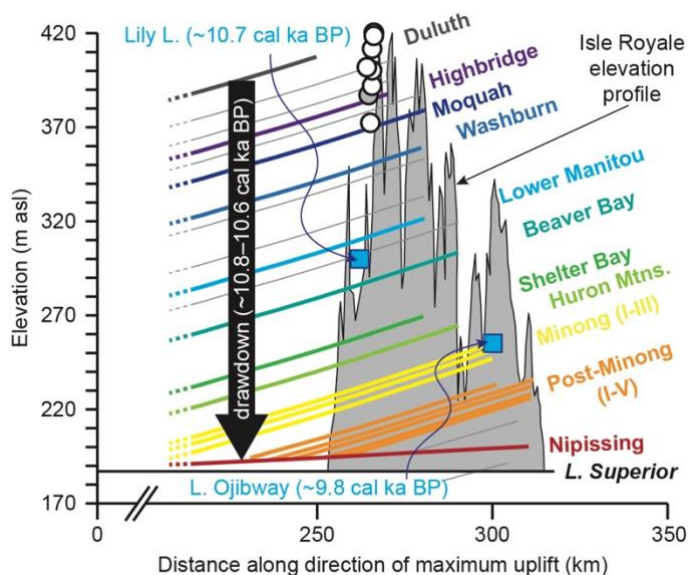
180 **Figure 4.** Elevation along topographic profile lines in Figure 3c: (A) Profile W; (B) Profile X; (C) Profile Y; (D) Profile Z. Elevation data comes from LiDAR imagery courtesy of Isle Royale National Park. Elevations of mapped strandlines are from Breckenridge (2013) and coloration of strandlines is same as in Figures 3; minor strandlines are indicated with gray dashed lines. Vertical exaggeration (VE) on each profile is indicated.

### 3 Methods

185 Samples were collected in 2018 from the tops of quartz-bearing glacial erratics situated on the highest-elevation recessional moraines on Isle Royale (Fig. 3; Table 1; Appendix A). Nine samples were collected from the Mt. Desor moraine (IR-18-01 through IR-18-09), one sample was positioned on the small Sugar Mtn. moraine (IR-18-10), and another (IR-18-11) was positioned on an upland till plain between the Sugar Mtn. and Mt. Desor moraines; since there are no known oral traditions or archival records of indigenous Ojibwemowin names for these moraines, we refer to them by their proximity to local geographic names. Sampled moraines are relatively higher than the surrounding landscape (Fig. 4) and targeting the highest-  
 190 elevation moraines on Isle Royale minimizes the potential of prolonged subaqueous erratic emplacement under lowering proglacial lake levels (Breckenridge, 2013). To this end, all samples collected are higher in elevation than Lily Lake, which was isolated from proglacial lakes in the Lake Superior basin by ~10.7 cal ka BP (median age; Flakne, 2003) while lake levels dropped from glacial Lake Duluth to post-Minong levels ~10.8–10.6 cal ka BP (Figs. 3, 4; median ages presented in



195 Breckenridge, 2013). If any of the samples were initially exposed from beneath retreating ice while underwater, they experienced less than ~100 yrs of subaqueous exposure, which is not long enough to significantly affect  $^{10}\text{Be}$  production and thus exposure ages. The tops of all erratics were >25 cm above the forest floor and eight of the eleven were >40 cm above the forest floor (Table 1).



200 **Figure 5.** Average elevation profile and traces of major strandlines identified on Isle Royale (adapted from Breckenridge, 2013). Drawdown of glacial Lake Duluth to Post-Minong stages, isolation of Lily Lake from proglacial lakes (blue square; median age; Flakne, 2003), and exposure of erratics used in this study (circles; gray circle is IR-18-11, which is not included in the mean age of deglaciation presented in this study) occurred within the ~200-year period from ~10.8–10.6 cal ka BP (median ages as presented in Breckenridge, 2013).

205

**Table 1. Sample Locations and Characteristics**

Sample ID	Latitude (°N)	Longitude (°W)	Elevation <sup>a</sup> (m)	Shielding	Thickness (cm)	Rock type	Dimensions L x W x H (cm)
IR-18-01	47.95536	89.01206	421	0.999997	2.0	Granite	80 x 80 x 35
IR-18-02	47.98524	89.01217	421	0.999998	3.0	Granite	90 x 70 x 25
IR-18-03	47.95000	89.01228	421	0.999996	3.3	Granite	135 x 110 x 30
IR-18-04	47.95499	89.01215	421	1.000000	1.5	Granite	130 x 110 x 40
IR-18-05	47.95890	89.01457	419	0.999771	4.3	Granite	130 x 80 x 50
IR-18-06	47.95174	89.02392	412	0.999998	2.0	Granite	240 x 150 x 40
IR-18-07	47.94902	89.02894	393	0.999872	2.5	Granite	270 x 190 x 75
IR-18-08	47.95077	89.02398	401	0.999805	1.5	Granite	265 x 240 x 65
IR-18-09	47.94488	89.03035	373	0.999781	3.0	Gneiss	150 x 120 x 65
IR-18-10	47.91520	89.06030	402	0.999999	2.8	Granite	145 x 150 x 60
IR-18-11	47.93444	89.04440	387	0.997475 <sup>b</sup>	3.8	Granite	250 x 200 x 75

<sup>a</sup> Elevations are present-day, meters above sea level, and are not corrected for glacial isostatic adjustment

<sup>b</sup> IR-18-11 was collected along the sloped top side of the erratic, which was adjacent to an even-larger mafic erratic. In addition to topographic shielding, shielding for IR-18-11 accounts for self-shielding of the erratic's sloped surface (strike 308°, dip 12°) and local horizon shielding from the adjacent erratic ([170°, 0.64], [180°, 0.86], [205°, 0.64]) using Balco et al.'s (2008) shielding calculator (wrapper 2.0, skyline 2.0).

Quartz was isolated from samples using froth-flotation and acid etching at the Purdue Rare Isotope Measurement (PRIME) Laboratory. Be was isolated and purified from quartz at the National Science Foundation / University of Vermont Community Cosmogenic Facility following established procedures (Corbett et al., 2016). We dissolved between 6.1 and 21.5 g of quartz and isotopically diluted each sample with  $\sim 250 \mu\text{g } ^9\text{Be}$  using an in-house carrier, termed UVM-SPEX, created from dilution of SPEX 10,000 ppm Be standard, with a resulting concentration of  $304 \mu\text{g mL}^{-1}$  (Table 2). The eleven samples were processed alongside one process blank.  $^{10}\text{Be}/^9\text{Be}$  ratios were measured at PRIME in March 2022 and normalized to primary standard 07KNSTD3110, with an assumed ratio of  $2.850 \times 10^{-12}$  (Nishiizumi et al., 2007). We corrected the measured  $^{10}\text{Be}/^9\text{Be}$  ratios with the ratio and uncertainty of the one process blank and propagated uncertainties in quadrature (Table 2).

Exposure ages of erratics were determined in February 2023 using Balco et al.'s (2008) exposure-age calculator (version 3, default production rate) based on present-day elevations, and Lifton et al.'s (2014) LSDn  $^{10}\text{Be}$  production rate scaling scheme. Topographic shielding for each sample was calculated in ArcGIS Pro using Li's (2018) point-based shielding tool and LiDAR imagery; the sloped surface of IR-18-11 required self-shielding calculations (see footnote in Table 1).  $^{10}\text{Be}$  exposure ages presented in this study assume no post-glacial erosion. Although a 70-yr monthly snowfall record exists for Isle Royale (Appendix B), its location is not near sampled sites, and it comprises  $<1\%$  of the duration of the Holocene, so we do not apply a snow shielding correction on reported ages. Erratic exposure via exhumation through degrading moraine crests is not considered to be significant on Isle Royale because the moraines are small ( $<30$  m in height), younger than the Younger Dryas, and are relatively prominent and geomorphically well-defined above the surrounding landscape, all of which greatly reduce the likelihood of long-term erratic exhumation (Putkonen and Swanson, 2003). The normality of the dataset was assessed using a Shapiro-Wilk  $W$  test in JMP software (vers. 16), and we subsequently use Chauvenet's Criterion to identify potential age outliers from the dataset (Clark et al., 2009; Rinterknecht et al., 2006).

## 230 4 Results

Measured concentrations of  $^{10}\text{Be}$  from the eleven erratics range from  $(3.98 \text{ to } 7.35) \times 10^4 \text{ atoms g}^{-1}$  (Table 2), which correspond to exposure ages of  $7.0 \pm 0.8 \text{ ka}$  to  $12.4 \pm 1.0 \text{ ka}$  ( $1\sigma$  internal uncertainties; Table 2; Fig. 6). Samples from the Mt. Desor moraine ( $n = 9$ ; IR-18-01 through IR-18-09) yield exposure ages ranging from  $9.0 \pm 0.7 \text{ ka}$  to  $12.4 \pm 1.0 \text{ ka}$  ( $1\sigma$ , internal). There is no relationship between erratic height above the surrounding landscape and exposure age ( $R^2 = 0.22$ ,  $p = 0.15$ ) and the fact that the lowest-lying erratic (IR-18-02, 25 cm) returns an exposure age that is older than the tallest two erratics (IR-18-07 and IR-18-11, 75 cm) suggests that erratics were not exposed by exhumation through degrading moraine crests. The exposure age dataset passes the Shapiro-Wilk test for normality ( $W = 0.92$ ;  $p = 0.35$ ), but one sample was identified as an outlier using Chauvenet's Criterion (IR-18-11). IR-18-11 was collected between the Mt. Desor and Sugar Mountain moraines, and we did not observe any evidence in the field of IR-18-11 having been rolled, tipped, buried, exhumed, or exposed due to

240 spalling in the past. The age of IR-18-11 places it out of chronological and geographic sequence between the otherwise similar exposure ages of erratics on the Mt. Desor and Sugar Mtn. moraines. As a result, we do not include IR-18-11 in subsequent statistics. After omitting the age of IR-18-11, the mean of ten samples from the Mt. Desor and Sugar Mtn. moraines is  $10.1 \pm 1.1$  ka (1 standard deviation (SD); Fig. 6).

245 Although all sampled erratics were chosen for the suitability for  $^{10}\text{Be}$  exposure age dating, and even though exposure ages are normally distributed, we present the mean age with one standard deviation uncertainties ( $\sim 11\%$  SD) because it is a conservative estimate that reflects the geological uncertainty of our samples and field area. The standard deviation of the mean age of our dataset is larger than the average shift in exposure ages that results from using any of the following: (i) a different exposure-age calculator (i.e. the Ice-TEA exposure age calculator; 6.7% shift; Jones et al., 2019), (ii) the Northeast North America  $^{10}\text{Be}$  production rate calibration (0.5% shift; Balco et al., 2009), (iii) a  $^{10}\text{Be}$  production rate scaling scheme other than LSDn (0.4% to 2.2% shift), (iv) glacial isostatic adjustments (Jones et al., 2019; 3.8% shift), or (v) snow shielding corrections (2.9% shift).  
 250 See Appendix B for details on age comparisons.

**Table 2.  $^{10}\text{Be}$  Isotopic Data and Exposure Ages**

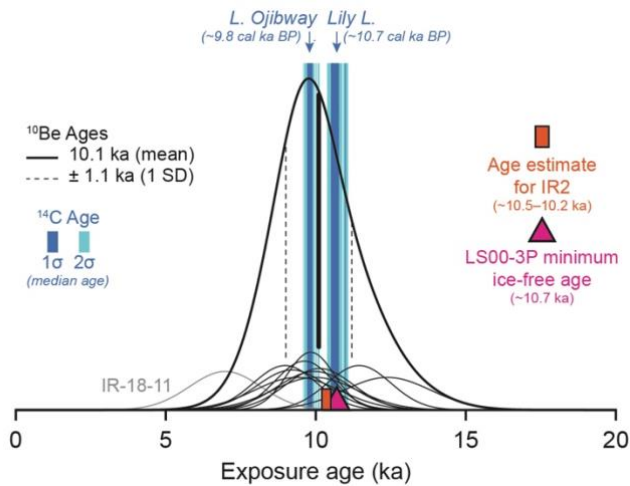
Sample Name	Quartz Mass (g)	Mass of $^9\text{Be}$ Added ( $\mu\text{g}$ ) <sup>a</sup>	AMS Cathode Number	Measured $^{10}\text{Be}/^9\text{Be}$ Ratio ( $\times 10^{-14}$ ) <sup>b</sup>	$\pm 1\sigma$ ( $\times 10^{-15}$ )	Background -Corrected		$^{10}\text{Be}$ (at $\text{g}^{-1}$ , $\times 10^6$ )	$\pm 1\sigma$ ( $\times 10^3$ )	Exposure Age (ka) <sup>d</sup>	$\pm 1\sigma$ (int/ex)
						$^{10}\text{Be}/^9\text{Be}$ Ratio ( $\times 10^{-14}$ ) <sup>c</sup>	$\pm 1\sigma$ ( $\times 10^{-15}$ )				
IR-18-01	8.508	250.1	162868	3.58	2.31	3.11	2.45	6.11	4.80	10.1	0.8/1.0
IR-18-02	12.503	251.2	162869	5.58	3.22	5.10	3.32	6.85	4.46	11.4	0.7/1.0
IR-18-03	10.028	250.3	162870	3.69	2.55	3.22	2.67	5.37	4.46	9.0	0.7/0.9
IR-18-04	7.995	251.2	162871	3.13	2.25	2.66	2.38	5.58	5.01	9.2	0.8/1.0
IR-18-05	6.133	250.7	162872	2.50	2.00	2.03	2.15	5.54	5.89	9.4	1.0/1.1
IR-18-06	7.156	250.2	162874	3.62	2.47	3.15	2.60	7.35	6.07	12.4	1.0/1.3
IR-18-07	6.730	250.7	162875	2.82	2.19	2.34	2.33	5.83	5.80	10.0	1.0/1.2
IR-18-08	10.057	249.7	162876	3.92	2.29	3.45	2.42	5.72	4.02	9.6	0.7/0.9
IR-18-09	21.500	250.4	162877	7.70	4.05	7.23	4.12	5.62	3.21	9.8	0.6/0.8
IR-18-10	8.333	250.9	162878	3.39	2.41	2.91	2.54	5.86	5.11	10.0	0.9/1.1
IR-18-11	8.287	249.2	162879	2.45	2.24	1.98	2.38	3.98	4.78	7.0	0.8/0.9

<sup>a</sup>  $^9\text{Be}$  was added using an in-house carrier, termed UVM-SPEX, created from dilution of SPEX 10,000 ppm Be standard, with a resulting concentration of  $304 \mu\text{g mL}^{-1}$ .

<sup>b</sup> Isotopic analysis was conducted at PRIME Laboratory on 8 March 2022; ratios were normalized against standard 07KNSTD3110 with an assumed ratio of  $2.850 \times 10^{-12}$  (Nishiizumi et al., 2007).

<sup>c</sup> Background corrections were made using one measurement blank sample. UVM Batch Number: 692; AMS Cathode Number: 162873; AMS  $^{10}\text{Be}/^9\text{Be}$  blank sample ratio:  $4.73\text{E-}15$ ;  $^{10}\text{Be}/^9\text{Be}$  blank sample ratio uncertainty:  $8.03\text{E-}16$ .

<sup>d</sup> Exposure ages calculated using in Balco et al.'s (2008) exposure age calculator (v. 3, default production rate), Lifton et al.'s (2014) scaling scheme (LSDn), a rock density of  $2.7 \text{ g cm}^{-3}$ , present-day elevations, topographic shielding (Li, 2018), and self-shielding for one sample (IR-18-11, Table 1). Other production rate calibrations, calculators, production rate scaling schemes, snow shielding, and glacial isostatic adjustment corrections were considered but ultimately not incorporated into the ages presented here (see Appendix B).



255

**Figure 6.** Distribution of  $^{10}\text{Be}$  exposure ages from this study (exclusive of IR-18-11; see Results). Ice-free conditions at Lily Lake and Lake Ojibway (Flakne, 2003) are shown by median  $^{14}\text{C}$  ages and their  $1\sigma$  and  $2\sigma$  distributions (dark and light blue, respectively;  $^{14}\text{C}$  age  $2\sigma$  ranges were recalibrated using CALIB rev. 8; Stuiver et al., 1993; median ages are unchanged from original publication). Minimum ice-free conditions southwest of Isle Royale at the LS00-3P core site (pink triangle) and the age estimates for the subaqueous IR2 moraine (orange rectangle) south of Isle Royale are also shown (Breckenridge, 2007; Colman et al., 2020).

260

## 5 Discussion

New  $^{10}\text{Be}$  ages of erratics from Isle Royale's Mt. Desor and Sugar Mountain moraines indicate they share a similar history of exposure at  $\sim 10.1 \pm 1.1$  ka (1 SD). This date provides new insights to the timing of LIS retreat from Isle Royale and the western Lake Superior basin following the Marquette Readvance (Fig. 7a). We interpret this age as the mean  $^{10}\text{Be}$  exposure age of the Mt. Desor and Sugar Mtn. moraines, recognizing that exposure ages of individual erratics, or the whole dataset could be shifted older if factors like snow shielding or exhumation could be reasonably accounted for. Exposure ages could likewise be shifted younger if our measurements include inherited  $^{10}\text{Be}$ , which is possible (Briner et al., 2016).

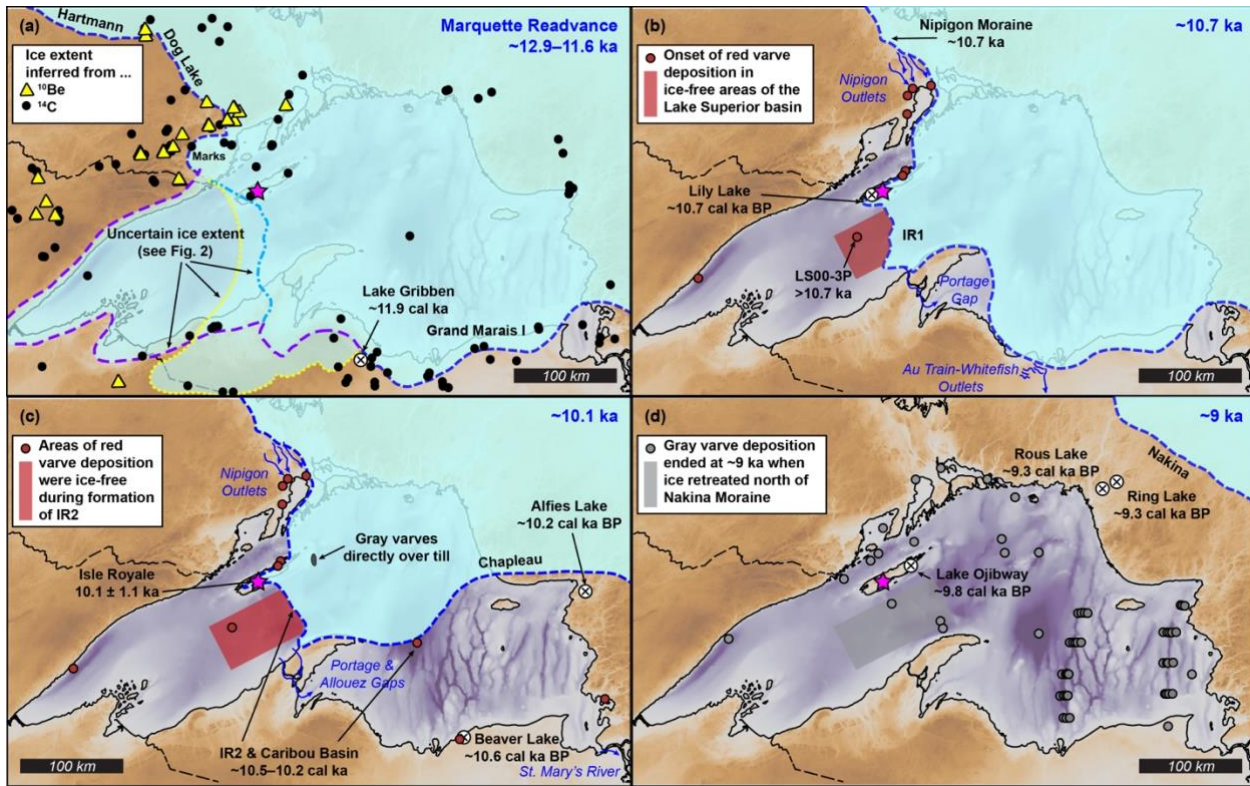
265

270

The  $^{10}\text{Be}$ -constrained timing of LIS retreat from the Mt. Desor and Sugar Mtn. moraines is chronologically and geographically consistent with the timeline of presently known deglaciation events on and around Isle Royale. For instance, the stratigraphy of the LS00-3P core southwest of Isle Royale has been interpreted to suggest ice-free conditions by  $\sim 10.7$  ka (Breckenridge, 2007), which is coeval with the timing of Lily Lake's isolation from proglacial lakes at  $\sim 10.7$  cal ka BP (minimum-limiting median age; 11.1–10.5 cal ka BP,  $2\sigma$  age range; Fig. 6; Flakne, 2003). The mean  $^{10}\text{Be}$  age of ice retreat from the Isle Royale's moraines ( $\sim 10.1$  ka) is consistent with the estimated timing of ice retreat from the subaqueous IR2 moraine south of Isle Royale ( $\sim 10.5$ – $10.2$  ka; Colman et al., 2020), which links the island to the Keweenaw Peninsula on the Michigan UP mainland. The earlier timing of ice-free conditions at the LS00-3P core and Lily Lake sites is reasonable given that they are positioned down ice of the Mt. Desor, Sugar Mtn., and subaqueous IR2 moraines. We take this regional

275

280 consistency among datasets to be an indication that, despite the 1.1 kyr uncertainty we report, the mean  $^{10}\text{Be}$  age of ice retreat of  $\sim 10.1$  ka is meaningful within the context of existing datasets and the deglaciation history of the western Lake Superior basin around Isle Royale.



285 **Figure 7.** Maps showing inferred Laurentide Ice Sheet margin positions at selected times: A.  $\sim 12.9$ – $11.6$  ka, during the Marquette Readvance (Dalton et al., 2020; Leydet et al., 2018; Lowell et al., 1999, 2005, 2009, 2021). B.  $\sim 10.7$  ka (Breckenridge, 2007; Flakne, 2003; Leydet et al., 2018; Lowell et al., 2021), when deposition of red varves are first observed across the western Lake Superior basin (Colman et al., 2020; Maher, 1977; Teller and Mahnic, 1988). C.  $\sim 10.1$  ka (this study), by which point, ice retreats north across the eastern Lake Superior basin (Breckenridge, 2007; Fisher and Whitman, 1999; Saarnisto, 1974), the transition from red to gray varve deposition occurs (Colman et al., 2020), and ice last traverses the western Lake Superior basin linking the North Shore with the Keweenaw Peninsula via Isle Royale (Colman et al., 2020; this study); ice continues to cover northern Lake Superior basin as indicated by gray varves directly over till (Mothersill and 290 Fun, 1982). D.  $\sim 9$  ka, by which point gray varves are ubiquitous across Lake Superior, terminating at  $\sim 9$  ka (Dell, 1976; Breckenridge 2007; Breckenridge et al., 2004; Colman et al., 2020; Fisher and Whitman, 1999; Halfman and Johnson, 1984; Hyoden and Longstaffe, 2011; Johnson and Fields, 1984; Maher, 1977; O’Beirne, 2013; Raymond et al., 1975; Teller and Mahnic, 1988; Yu et al., 2010). Minimum-limiting ages (cal ka BP) of Rous Lake and Ring Lake are median ages of organic 295 sediment (Bajc et al., 1997; Saarnisto, 1974). Background imagery is 3 arcsecond Bathymetry of Lake Superior dataset, which shows elevations in meters above sea level and depths below present-day lake level (NOAA Great Lakes Environmental Research Lab, 1999); color shading for the background imagery is the same as in Fig. 2.

300

Based on the similarity between the mean  $^{10}\text{Be}$  age of Isle Royale's moraines reported here (~10.1 ka) and the age of formation of the subaqueous IR2 moraine south of the island (~10.5–10.2 ka; Colman et al., 2020), we suggest that LIS retreat from the western Lake Superior basin south of the island occurred later than it did along Lake Superior's North Shore (~10.7 ka; mean of  $^{10}\text{Be}$  ages from the Nipigon Moraine and nearest sites west of Lake Nipigon; Fig. 7; Leydet et al., 2018; Lowell et al., 2021) as these sample sites and ours are likely to share similar snow cover and inheritance histories. Nearly-constant modelled ice retreat rates of ~40–60 m yr<sup>-1</sup> are reported along Lake Superior's North Shore (Lowell et al., 2021); a similar retreat rate of ~45 m yr<sup>-1</sup> can be inferred between Lily Lake and Lake Ojibway on Isle Royale (~42 km) from minimum-limiting  $^{14}\text{C}$  bulk-sediment ages (Fig. 3, Flakne, 2003). However, ice retreat south of Isle Royale from the LS00-3P core site (~10.7 ka; Fig. 2; Breckenridge, 2007) to the Mt. Desor and IR2 moraines (~10.1 ka; ~60 km; Colman et al., 2020; this study) indicates a mean ice retreat rate of ~100 m yr<sup>-1</sup>. Although the ice retreat rate south of Isle Royale appears to outpace the North Shore retreat rate and that between inland lakes on Isle Royale, ice retreat south of the island must have paused long enough to construct the ≤20 m high subaerial Mt. Desor moraines (profile X, Fig. 4) and the ~60–100 m high subaqueous IR1 and IR2 moraines during a time when proglacial lake levels were similar to those of glacial Lake Duluth (Colman et al., 2020).

Subaqueous moraines were not identified in Lake Superior north of Isle Royale during multiple seismic surveys (Colman et al., 2020; Johnson, 1980; Landmesser et al., 1982). Neither the ~45 m yr<sup>-1</sup> retreat rate between Isle Royale's inland lakes nor the ~100 m yr<sup>-1</sup> retreat rate south of Isle Royale we infer based on new  $^{10}\text{Be}$  exposure ages account for periods of standstill during which time these large moraines were constructed. Therefore, the estimates of ice retreat south of Isle Royale should be considered minimum average retreat rates, with rapid retreat before and after periods of standstill, perhaps being facilitated by high rates of iceberg calving over deeper water (Colman et al., 2020). This interpretation of ages and retreat rates in the western Lake Superior basin supports the previously proposed hypothesis that the topography of Isle Royale and the Keweenaw Peninsula provided lateral stability to the retreating ice margin in relatively shallow waters, which delayed its overall retreat, relative to ice retreat long the North Shore (Colman et al., 2020).

Early work, based on the relative positions of subglacial, ice marginal, and proglacial landforms on Isle Royale, suggests that moraines on Isle Royale formed in a subaerial environment, likely associated with the Beaver Bay stage of glacial Lake Duluth (Huber, 1973). The mean  $^{10}\text{Be}$  exposure age (~10.1 ka), however, implies that moraine exposure may have been later, postdating the drawdown of glacial Lake Duluth beyond the Beaver Bay stage, at least to post-Minong stages (~10.8–10.6 cal ka BP, median ages; Breckenridge, 2013). In support of this reinterpretation is the observation that strandlines of early proglacial lakes (e.g. Highbridge to Shelter Bay; Figs. 3b, 4) are present at high elevations on the island, but only on northwest-facing slopes, whereas strandlines of younger proglacial lakes (e.g. Huron Mtn. and younger; Figs. 3b, 4) are found on northwest- and southeast-facing slopes at lower elevations (Breckenridge, 2013; Farrand, 1969). All striae, craig-and-tail structures, and ice-marginal landforms are found at elevations above the younger strandlines and were thus formed by ice that covered southeast-facing slopes late into the drawdown history of proglacial lakes (Huber, 1973). Similarly, strandlines older

335 than post-Minong stages appear to be absent from northwest-facing slopes on the Keweenaw Peninsula across from Isle Royale  
(Breckenridge, 2013), though they do exist down-ice of the IR1 moraine (Hughes, 1963).

The apparent absence of strandlines older than post-Minong on southeast-facing slopes on Isle Royale and northwest-facing  
slopes along the Keweenaw Peninsula further points to long-lasting ice cover between the two landforms until ice retreat in  
340 the early Holocene. Post-Minong and younger strandlines are found along Isle Royale, including northeast (up ice) of mapped  
moraines. The emergence of Lake Ojibway on Isle Royale's northeast end at ~9.8 cal ka BP (minimum-limiting median age;  
10.1–9.7 cal ka BP,  $2\sigma$  age range, Flakne, 2003) places a minimum age limit on ice retreat from the island's moraines and the  
subaqueous IR2 moraine. Together, these ages imply that the timing of LIS retreat from Isle Royale's moraines, abandonment  
of the IR2 moraine, and the presence of post-Minong stages of glacial Lake Duluth are roughly coeval sometime between  
345 ~10.6–10.1 ka (Breckenridge, 2013; Colman et al., 2020; this study).

Division of the retreating LIS margin into two separate retreating fronts, northwest and southeast of Isle Royale in the early  
Holocene has implications for meltwater routing and the Lake Superior lake-bottom stratigraphy. Red varves associated with  
influx of meltwater from glacial Lake Agassiz (Breckenridge et al., 2004) were identified down-ice of the subaqueous IR2  
350 moraine south of Isle Royale, but not up-ice (Fig. 2B), and Colman et al. (2020) interpreted this to mean gray varve deposition  
across Lake Superior was associated specifically with ice retreat from the IR2 moraine, not from the Lake Superior basin itself  
(Farrand, 1969). Following Colman et al.'s (2020) interpretation, the similar ages of Isle Royale's recessional moraines and  
IR2 implies that the presence and absence of red varves across the Lake Superior basin delineates a regional ice margin when  
ice was last present on Isle Royale. Previously drawn maps place the LIS margin across the northern Lake Superior basin by  
355 ~10.5 ka (Fig. 2; Breckenridge, 2007), but red varves do not appear to be present in Nipigon Bay nor the northern Lake Superior  
basin, and gray varves are identified directly overlying till (i.e. no red varves) at a shallow rise northeast of Isle Royale (Fig.  
2; Mothersill and Fung, 1972).

The absence of red varves in the northern Lake Superior basin is most likely a result of earlier ice retreat to the Nipigon moraine  
360 by ~10.7 ka north of Isle Royale (Leydet et al., 2018; Lowell et al., 2021) where the ice margin paused in its retreat along the  
divide between Black Bay and Nipigon Bay (Fig. 7b; Teller and Mahnic, 1988). We suggest that water in the western Lake  
Superior basin was blocked from draining north around both Isle Royale and the Keweenaw Peninsula by the presence of ice  
spanning from the Keweenaw Peninsula to the Nipigon moraine via the outer subaqueous IR1 moraine and Isle Royale (Fig.  
7b).

365 In this case, the initial influxes of meltwater from glacial Lake Agassiz, which carried the reddish varve-forming sediment,  
would have first drained into the western Lake Superior basin at Black Bay and then drained across the Keweenaw Peninsula  
to the eastern Lake Superior basin via the Portage and Allouez outlets (Fig. 7b, c). The Portage and Allouez Gaps are known

370 to have previously carried water, but neither have been dated (Hughes, 1963), and we propose that these outlets were  
abandoned following the rapid ice retreat from Isle Royale and IR2 after ~10.1 ka (Fig. 7d). Ice retreat from Michigan's UP in  
the eastern Lake Superior basin occurred by ~10.5–10.2 ka (Breckenridge, 2007; Fisher and Whitman, 1999) and quickly  
retreated north, perhaps to the vicinity of the Chapleau moraine ~10.2 ka (Saarnisto et al., 1974).

375 Following retreat from Isle Royale and the IR2 moraine, the LIS ice retreated to the Nakina Moraine, exposing the entirety of  
the northern Lake Superior basin and small lakes between Lake Superior's North Shore and the Nakina Moraine in less than 1  
ky (Fig. 7d; Bajc et al., 1997; Breckenridge 2007, 2013; Breckenridge et al., 2004; Colman et al., 2020; Hyodo and Longstaffe,  
2011; Kelly et al., 2016; Lowell et al., 2021; Saarnisto, 1974; Teller and Mahnic, 1988). During this retreat, gray varves were  
deposited across all of the Lake Superior basin, terminating in a series of 36 anomalously thick varves that are associated with  
380 7). This inferred retreat timing, extrapolated over the >300 km distance from Isle Royale and the IR2 moraine to the Nakina  
moraine, means ice retreat rates south of Isle Royale nearly tripled to a mean retreat rate of ~270 m yr<sup>-1</sup> as the ice margin  
retreated across deep waters of northern Lake Superior. This rapid retreat accounts for the lack of glacial deposits on the  
northeastern-most two thirds of Isle Royale where Precambrian bedrock is exposed (Fig. 3; Huber, 1973).

## 6 Implications

385 The interpretations we draw from <sup>10</sup>Be exposure ages from recessional moraines on Isle Royale provide new, quantitative  
constraints on the timing of ice retreat from Isle Royale. These new <sup>10</sup>Be exposure ages from within Lake Superior expand  
the geographical coverage of quantitative age constraints on the timing of LIS retreat from the Great Lakes. By inferring that  
subaerial moraine construction on Isle Royale is contemporaneous with subaqueous moraine construction between Isle  
Royale and Michigan's Keweenaw Peninsula, we show that the spatial distribution of red varves throughout the Lake  
390 Superior basin can be used to delineate the position of the LIS margin in the early Holocene. In doing so, we provide support  
for the notion that southern margins of the LIS remaining in contact with the southern shores of Lake Superior into the early  
Holocene prior to its final and rapid retreat. Interpreting our new <sup>10</sup>Be based chronology of ice retreat from Isle Royale  
within the spatial and geomorphological context of existing proglacial and subglacial landforms and stratigraphy bridges  
existing ice retreat chronologies along Lake Superior's North Shore with the Lake Superior south shore along the Keweenaw  
395 Peninsula. Interpretations drawn from the dataset presented here demonstrate that dating glacial features on islands can be  
integral to reconstructing regional patterns of deglaciation across bodies of water and drawing relationships between  
subaerial and subaqueous glacial landforms and regional stratigraphy.



## Appendix A: Photographs of sample sites

400 Glacial erratics are common across Isle Royale. Those suitable for  $^{10}\text{Be}$  exposure age dating are easily identifiable because they are often granite or metamorphic rocks from the Canadian Shield, which stand in stark contrast to the mafic igneous and volcaniclastic rocks comprising the bedrock of Isle Royale. Most erratics are smaller than those typically found in Alpine environments because of the long transport distances from their sources. During the three days of fieldwork on Isle Royale, many erratics were identified but only those most suitable for dating were sampled. Sampled erratics were those positioned  
405 on moraine crests or broad uplands with minimal topographic shielding and least likely to have rolled down hills or have complex exposure and/or burial histories (Fig. A1).



410 **Figure A1.** Photographs of the eleven samples used in this study. Rock hammers, plastic zip bags, GPS units, and people are present for scale.

## Appendix B: Sensitivity analyses of exposure-age calculation decisions

In this study, we present exposure ages that were calculated using the online exposure-age calculator presented by Balco et al. (2008; vers. 3) using the default  $^{10}\text{Be}$  production rate calibration and the LSDn  $^{10}\text{Be}$  production rate scaling scheme (Lifton et al., 2014). Standard  $^{10}\text{Be}$  production shielding corrections were made (Table 1), but we do not incorporate any  
415 other production rate scaling options nor use a regional  $^{10}\text{Be}$  calibration dataset. In each section of Appendix B, we explore

how  $^{10}\text{Be}$  exposure ages from Isle Royale would have shifted had we made different decisions. Importantly, calculating ages with any of these adjustments only results in minor changes in exposure ages and would not alter the results of this study.

## B.1 Choice of exposure-age calculator

420 We considered the use of two online calculators, the first presented by Balco et al. (2008), which is regularly updated, and  
 the newer Ice-TEA calculator (Jones et al., 2019). Both calculators follow the guiding principles of cosmogenic nuclide  
 production (Gosse and Phillips, 2001), but with recognized differences, including how atmospheric pressure is incorporated  
 into age calculations or how easily users can choose regional production rate calibration datasets. Differences in calibration  
 425 datasets have led to differences in exposure ages from the same input data for at least one previous study in the Great Lakes  
 region (e.g. Lowell et al., 2021). In this study, exposure ages calculated with the Ice-TEA calculator are, on average, 6.7%  
 older (range: 5.8% to 7.0%) than ages calculated using Balco et al.'s calculator (Table B1). We chose to present ages from  
 Balco et al. (2008)'s calculator, primarily because of its longevity and because it is used by other  $^{10}\text{Be}$  exposure-age studies  
 in the Great Lakes region.

**Table B1. Exposure ages calculated using Balco et al. (2008) versus Ice-TEA**

Sample ID	Balco et al. (2008)			Ice-TEA (Jones et al., 2019)			% diff.
	Age (ka)	$\pm 1\sigma$ (int.)	$\pm 1\sigma$ (ext.)	Age (ka)	$\pm 1\sigma$ (int.)	$\pm 1\sigma$ (ext.)	
IR-18-01	10126	798	998	10820	940	1260	6.9%
IR-18-02	11446	747	1009	12250	790	1250	7.0%
IR-18-03	8979	748	917	9580	830	1110	6.7%
IR-18-04	9207	828	991	9820	910	1220	6.7%
IR-18-05	9374	998	1142	10020	1080	1350	6.9%
IR-18-06	12385	1025	1260	13140	1100	1470	6.1%
IR-18-07	9973	994	1156	10660	1080	1370	6.9%
IR-18-08	9619	677	884	10280	760	1090	6.9%
IR-18-09	9831	562	809	10510	590	1010	6.9%
IR-18-10	9954	870	1051	10630	970	1290	6.8%
IR-18-11	6982	841	937	7390	860	1030	5.8%

430

## B.2 Choice of $^{10}\text{Be}$ production rate calibration

Previous  $^{10}\text{Be}$  exposure-age studies in the Great Lakes region (e.g. Leydet et al., 2018; Lowell et al., 2021) used the  
 Northeast North America (NENA) calibration for  $^{10}\text{Be}$  production rates (Balco et al., 2009), which results in exposure ages  
 that are each 0.5% younger than those we use in determining the mean exposure age of deglaciation from Isle Royale (Table  
 435 B2). Although the samples we collected from Isle Royale are ice-marginal landforms found at relative high latitudes (~48°N)  
 and at elevations <1,000 m asl, we use the default  $^{10}\text{Be}$  calibration production rate in our age calculations using Balco et al.'s  
 (2008) calculator, primarily because of our distance from NENA calibration sites.

**Table B2. Exposure ages calculated in Balco et al. (2008) using the default versus Northeast North America calibration datasets**

Sample ID	Default production rate calibration			Northeast North America calibration			% diff.
	Age (ka)	$\pm 1\sigma$ (int.)	$\pm 1\sigma$ (ext.)	Age (ka)	$\pm 1\sigma$ (int.)	$\pm 1\sigma$ (ext.)	

IR-18-01	10126	798	998	10079	795	1157	0.5%
IR-18-02	11446	747	1009	11389	744	1207	0.5%
IR-18-03	8979	748	917	8936	744	1053	0.5%
IR-18-04	9207	828	991	9164	824	1124	0.5%
IR-18-05	9374	998	1142	9330	993	1262	0.5%
IR-18-06	12385	1025	1260	12318	1020	1448	0.5%
IR-18-07	9973	994	1156	9925	989	1290	0.5%
IR-18-08	9619	677	884	9572	674	1045	0.5%
IR-18-09	9831	562	809	9783	560	990	0.5%
IR-18-10	9954	870	1051	9906	866	1197	0.5%
IR-18-11	6982	841	937	6950	837	1018	0.5%

440

### B.3 Choice of $^{10}\text{Be}$ production rate scaling scheme

Previous studies present exposure ages using different production rate scaling schemes including non-time-dependent scaling based on atmospheric measurements (St; Lal, 1991; Stone, 2000) and time-dependent scaling based on atmospheric measurements and paleomagnetic reconstructions (Lm; Lal, 1991; Nishiizumi et al., 1989; Stone, 2000). Our preference of  $^{10}\text{Be}$  production rate scaling is to use Lifton et al.'s (2014) LSDn scaling scheme because it accounts for changes in the strength of Earth's magnetosphere, changes in solar cosmic ray output, and numerous cosmogenic isotope production pathways (LSDn; Lifton et al., 2014). Exposure ages of erratics on Isle Royale based on non-time-dependent spallogenic scaling (St) are on average 0.4% older (range: 0.2% to 0.7%) and exposure ages based on time-dependent spallogenic scaling (Lm) are on average 2.2% younger (range: 2.0% to 2.8%) than ages derived using Lifton et al.'s (2014) LSDn scaling scheme (Table B3).

**Table B3. Exposure ages calculated in Balco et al. (2008) using difference  $^{10}\text{Be}$  production rate scaling schemes**

Sample ID	LSDn			St			% diff.	Lm			% diff.
	Age (ka)	$\pm 1\sigma$ (int.)	$\pm 1\sigma$ (ext.)	Age (ka)	$\pm 1\sigma$ (int.)	$\pm 1\sigma$ (ext.)		Age (ka)	$\pm 1\sigma$ (int.)	$\pm 1\sigma$ (ext.)	
IR-18-01	10126	798	998	10156	801	1135	0.3%	9911	781	1080	2.1%
IR-18-02	11446	747	1009	11483	750	1179	0.3%	11186	730	1114	2.3%
IR-18-03	8979	748	917	9015	751	1036	0.4%	8797	733	987	2.0%
IR-18-04	9207	828	991	9238	831	1107	0.3%	9017	811	1057	2.1%
IR-18-05	9374	998	1142	9405	1001	1248	0.3%	9180	977	1196	2.1%
IR-18-06	12385	1025	1260	12328	1021	1413	0.5%	12039	997	1347	2.8%
IR-18-07	9973	994	1156	9996	996	1273	0.2%	9755	972	1218	2.2%
IR-18-08	9619	677	884	9657	680	1023	0.4%	9428	664	971	2.0%
IR-18-09	9831	562	809	9856	564	963	0.3%	9621	550	909	2.1%
IR-18-10	9954	870	1051	9978	872	1177	0.2%	9736	851	1123	2.2%
IR-18-11	6982	841	937	6936	835	1000	0.7%	6794	818	964	2.7%

### B.4 Effects of snow shielding

Previous  $^{10}\text{Be}$  studies in the region used sample collection strategies to minimize the potential of snow-shielding (e.g. unforested, windswept, high-elevation locations; Leydet et al., 2018; Lowell et al., 2021); this was not an option on Isle Royale.

Given its position in the middle of Lake Superior, heavy lake effect snow is probable on Isle Royale, and the forest at the Mt. Desor and Sugar Mountain Moraines may prevent fallen snow from blowing away easily. We considered the effects of snow-shielding at our sample sites using average monthly snow-depth totals that were measured at Isle Royale’s Mott Island Station:

- 460
- Station: #205637 (National Climatic Data Center, NCDC)
  - Location: 48°06’ N, 88°33’ W
  - Elevation: 610 ft above sea level
  - Period of record: 01 October 1940 to 29 April 2016 (41.8% of possible observations reported, Table B4)
  - Data access: Western Regional Climate Center, <https://wrcc.dri.edu/> (last accessed 22 February 2023)

465 Snow shielding calculations are based on Eq. (3.76) in Gosse and Phillips (2001):

$$S_{snow} = \frac{1}{12} \sum_i^{12} e^{-(z_{snow,i} \rho_{snow,i} / \Lambda)},$$

Here,  $z_{snow,i}$  is the monthly average snow thickness above the ground (cm),  $\rho_{snow,i}$  is the monthly average snow density (g cm<sup>-3</sup>), and  $\Lambda$  is attenuation of cosmic rays (160 g cm<sup>-2</sup>). We use an average old-age snow density of 0.27 g cm<sup>-3</sup> measured from  
470 Isle Royale (Peterson, 1977).

**Table B4. Monthly average snow depth at Mott Island (October 1940–April 2016)**

	Jan	Feb	Mar	Apr	May	Jun	Jul	Aug	Sep	Oct	Nov	Dec
<b>Reported (inches)</b>	13	23	25	10	0	0	0	0	0	0	2	8
<b>For shielding calculations (cm)</b>	33.0	58.4	63.5	25.4	0	0	0	0	0	0	5.1	20.3

Including snow shielding led to exposure ages that were, on average, 2.9% older (range: 2.6% to 3.3%) than without snow shielding (Table B5). We choose not to include these ages in our analysis because measured snowfall from 1940 to 2016  
475 may not accurately reflect Holocene averages.

**Table B5. Exposure ages calculated in Balco et al. (2008) without versus with snow shielding**

Sample ID	Without snow shielding			With snow shielding			% diff.
	Age (ka)	± 1σ (int.)	± 1σ (ext.)	Age (ka)	± 1σ (int.)	± 1σ (ext.)	
IR-18-01	10126	798	998	10413	821	1026	2.8%
IR-18-02	11446	747	1009	11793	770	1039	3.0%
IR-18-03	8979	748	917	9238	769	944	2.9%
IR-18-04	9207	828	991	9463	851	1019	2.8%
IR-18-05	9374	998	1142	9630	1025	1173	2.7%
IR-18-06	12385	1025	1260	12791	1059	1302	3.3%
IR-18-07	9973	994	1156	10254	1022	1189	2.8%
IR-18-08	9619	677	884	9903	697	911	3.0%
IR-18-09	9831	562	809	10113	579	832	2.9%
IR-18-10	9954	870	1051	10234	895	1080	2.8%
IR-18-11	6982	841	937	7167	863	962	2.6%

## B.5 Effects of glacial isostatic adjustment

480 Sample sites in this study are ~300 km up-ice of the Laurentide Ice Sheet's Last Glacial Maximum terminal moraines  
(Ullman et al., 2015) and strandlines of proglacial lakes that once occupied the western Lake Superior basin have  
experienced considerable uplift (Breckenridge, 2013; Farrand, 1969). In considering the effects of glacial isostatic  
adjustment (GIA) on the exposure ages presented in this study, we compare exposure ages from all samples using only the  
Ice-TEA software package's "Correct for Elevation Change" tool and the ICE-6G GIA model (Jones et al., 2019; Peltier et  
al., 2015). GIA-corrected ages are compared to uncorrected ages. Exposure ages with GIA-corrections were on average 3.8%  
485 older (range: 1.1% to 8.1%) than exposure ages uncorrected for GIA (Table B6). Following Lowell et al. (2021), we choose  
to use exposure ages uncorrected for GIA to maintain regional comparability of exposure-age datasets.

**Table B6. Exposure ages calculated in Ice-TEA without versus with glacial isostatic adjustment corrections**

Sample ID	Without GIA adjustment		With GIA adjustment		% diff.
	Age (ka)	$\pm 1\sigma$ (int.)	Age (ka)	$\pm 1\sigma$ (int.)	
IR-18-01	10820	940	11240	1430	3.9%
IR-18-02	12250	790	13020	1600	6.3%
IR-18-03	9580	830	9830	1280	2.6%
IR-18-04	9820	910	10110	1300	3.0%
IR-18-05	10020	1080	10310	1470	2.9%
IR-18-06	13140	1100	14210	2060	8.1%
IR-18-07	10660	1080	11060	1560	3.8%
IR-18-08	10280	760	10610	1230	3.2%
IR-18-09	10510	590	10880	1230	3.5%
IR-18-10	10630	970	11020	1450	3.7%
IR-18-11	7390	860	7470	1020	1.1%

### Data Availability

490 All data required to reproduce the results and analyses of this study are presented in data tabled herein. Topographic  
shielding was done using LiDAR elevation datasets provided by Seth DePasqual with the US National Park Service.

### Sample Availability

All sample material removed from Isle Royale National Park was destroyed in sample preparation and  $^{10}\text{Be}$  extraction at  
Purdue University's PRIME lab and the University of Vermont Community Cosmogenic Facility.

### 495 Author Contribution

EWP: Conceptualization, formal analysis, funding acquisition, investigation, project administration, visualization, writing –  
original draft preparation. DJU: Formal analysis, investigation, photographs, writing – original draft preparation. LBC: Data  
curation, formal analysis, investigation, writing – original draft preparation. PRB: Formal analysis, investigation, resources,  
writing – original draft preparation. MC: Data curation, funding acquisition, resources, writing – original draft preparation.

## Competing Interests

The authors declare that they have no conflict of interest.

## Acknowledgements

- 505 This study was conducted on Isle Royale, which is a Traditional Cultural Property of the Grand Portage Band of Lake Superior  
Chippewa, who call the island, “Minong.” We thank Erik Redix and Tim Cochrane for advice us on indigenous place-names  
for the Mt. Desor and Sugar Mtn. moraines. Ojibwemowin names are presently unknown for these sites. We thank Mark  
Romanski and Seth Depasqual from Isle Royale National Park for providing sample collection permit approval and LiDAR  
510 imagery, respectively. Stephen Ogden helped with sample collection. Funding for this project was through an Eastern Michigan  
University Faculty Research Fellowship and a PRIME Laboratory Seed Data Grant, both awarded to EWP. Sample processing  
at the NSF/UVM CCF supported by NSF EAR-1735676.

## References

- Bajc, A. F., Morgan, A. V., and Warner, B. G.: Age and paleoecological significance of an early postglacial fossil  
assemblage near Marathon, Ontario, Canada, *Can. J. Earth Sci.*, 34, 687–698, <https://doi.org/10.1139/e17-055>, 1997.
- 515 Balco, G., Briner, J., Finkel, R. C., Rayburn, J. A., Ridge, J. C., and Schaefer, J. M.: Regional beryllium-10 production rate  
calibration for late-glacial northeastern North America, *Quaternary Geochronology*, 4, 93–107,  
<https://doi.org/10.1016/j.quageo.2008.09.001>, 2009.
- Balco, G., Stone, J. O., Lifton, N. A., and Dunai, T. J.: A complete and easily accessible means of calculating surface  
520 exposure ages or erosion rates from  $^{10}\text{Be}$  and  $^{26}\text{Al}$  measurements, *Quaternary Geochronology*, 3, 174–195,  
<https://doi.org/10.1016/j.quageo.2007.12.001>, 2008.
- Black, R. F.: Quaternary geology of Wisconsin and contiguous Upper Michigan, in: *Quaternary stratigraphy of North  
America*, edited by: Mahaney, W. C., Dowden, Hutchinson & Ross ; exclusive distributor, Halsted Press, Stroudsburg,  
Pa. : [New York], 1976.
- Borchers, B., Marrero, S., Balco, G., Caffee, M., Goehring, B., Lifton, N., Nishiizumi, K., Phillips, F., Schaefer, J., and  
525 Stone, J.: Geological calibration of spallation production rates in the CRONUS-Earth project, *Quaternary  
Geochronology*, 31, 188–198, <https://doi.org/10.1016/j.quageo.2015.01.009>, 2016.
- Breckenridge, A., Lowell, T. V., Peteet, D., Wattrus, N., Moretto, M., Norris, N., and Dennison, A.: A new glacial varve  
chronology along the southern Laurentide Ice Sheet that spans the Younger Dryas–Holocene boundary, *Geology*, 49,  
283–288, <https://doi.org/10.1130/G47995.1>, 2021.
- 530 Breckenridge, A.: An analysis of the late glacial lake levels within the western Lake Superior basin based on digital  
elevation models, *Quaternary Research*, 80, 383–395, <https://doi.org/10.1016/j.yqres.2013.09.001>, 2013.
- Breckenridge, A.: The Lake Superior varve stratigraphy and implications for eastern Lake Agassiz outflow from 10,700 to  
8900 cal ybp (9.5–8.0  $^{14}\text{C}$  ka), *Palaeogeography, Palaeoclimatology, Palaeoecology*, 246, 45–61,  
<https://doi.org/10.1016/j.palaeo.2006.10.026>, 2007.
- 535 Breckenridge, A.: The timing of regional Lateglacial events and post-glacial sedimentation rates from Lake Superior,  
*Quaternary Science Reviews*, 23, 2355–2367, <https://doi.org/10.1016/j.quascirev.2004.04.007>, 2004.
- Briner, J. P., Goehring, B. M., Mangerud, J., and Svendsen, J. I.: The deep accumulation of  $^{10}\text{Be}$  at Utsira, southwestern  
Norway: Implications for cosmogenic nuclide exposure dating in peripheral ice shee landscapes, *Geophysical Research  
Letters*, 43, 9121–9129, <https://doi.org/10.1002/2016GL070100>, 2016.
- 540 Broecker, W. S., Kennett, J. P., Flower, B. P., Teller, J. T., Trumbore, S., Bonani, G., and Wolfli, W.: Routing of meltwater  
from the Laurentide Ice Sheet during the Younger Dryas cold episode, *Nature*, 341, 318–321,  
<https://doi.org/10.1038/341318a0>, 1989.

- Broecker, W. S.: Was the Younger Dryas Triggered by a Flood?, *Science*, 312, 1146–1148, <https://doi.org/10.1126/science.1123253>, 2006.
- 545 Carlson, A. E., Clark, P. U., Haley, B. A., Klinkhammer, G. P., Simmons, K., Brook, E. J., and Meissner, K. J.: Geochemical proxies of North American freshwater routing during the Younger Dryas cold event, *Proc. Natl. Acad. Sci. U.S.A.*, 104, 6556–6561, <https://doi.org/10.1073/pnas.0611313104>, 2007.
- Carlson, A. E.: What Caused the Younger Dryas Cold Event?, *Geology*, 38, 383–384, <https://doi.org/10.1130/focus042010.1>, 2010.
- 550 Ceperley, E. G., Marcott, S. A., Rawling, J. E., Zoet, L. K., and Zimmerman, S. R. H.: The role of permafrost on the morphology of an MIS 3 moraine from the southern Laurentide Ice Sheet, *Geology*, 47, 440–444, <https://doi.org/10.1130/G45874.1>, 2019.
- Clark, P. U. and Mix, A. C.: Ice sheets and sea level of the Last Glacial Maximum, *Quaternary Science Reviews*, 21, 1–7, [https://doi.org/10.1016/S0277-3791\(01\)00118-4](https://doi.org/10.1016/S0277-3791(01)00118-4), 2002.
- 555 Clark, P. U., Dyke, A. S., Shakun, J. D., Carlson, A. E., Clark, J., Wohlfarth, B., Mitrovica, J. X., Hostetler, S. W., and McCabe, A. M.: The Last Glacial Maximum, *Science*, 325, 710–714, <https://doi.org/10.1126/science.1172873>, 2009.
- Clayton, L. and Moran, S. R.: Chronology of late wisconsinan glaciation in middle North America, *Quaternary Science Reviews*, 1, 55–82, [https://doi.org/10.1016/0277-3791\(82\)90019-1](https://doi.org/10.1016/0277-3791(82)90019-1), 1982.
- 560 Colgan, P. M., Bierman, P. R., Mickelson, D. M., and Caffee, M.: Variation in glacial erosion near the southern margin of the Laurentide Ice Sheet, south-central Wisconsin, USA: Implications for cosmogenic dating of glacial terrains, *Geological Society of America Bulletin*, 114, 1581–1591, [https://doi.org/10.1130/0016-7606\(2002\)114<1581:VIGENT>2.0.CO;2](https://doi.org/10.1130/0016-7606(2002)114<1581:VIGENT>2.0.CO;2), 2002.
- Colman, S. M., Breckenridge, A., Zoet, L. K., Wattrus, N. J., and Johnson, T. C.: Moraines and late-glacial stratigraphy in central Lake Superior, *Quat. res.*, 98, 19–35, <https://doi.org/10.1017/qua.2020.36>, 2020.
- 565 Corbett, L. B., Bierman, P. R., and Rood, D. H.: An approach for optimizing in situ cosmogenic <sup>10</sup>Be sample preparation, *Quaternary Geochronology*, 33, 24–34, <https://doi.org/10.1016/j.quageo.2016.02.001>, 2016.
- Cutler, P. M., Mickelson, D. M., Colgan, P. M., MacAyeal, D. R., and Parizek, B. R.: Influence of the Great Lakes on the dynamics of the southern Laurentide ice sheet: Numerical experiments, *Geol*, 29, 1039, [https://doi.org/10.1130/0091-7613\(2001\)029<1039:IOTGLO>2.0.CO;2](https://doi.org/10.1130/0091-7613(2001)029<1039:IOTGLO>2.0.CO;2), 2001.
- 570 Dalton, A. S., Margold, M., Stokes, C. R., Tarasov, L., Dyke, A. S., Adams, R. S., Allard, S., Arends, H. E., Atkinson, N., Attig, J. W., Barnett, P. J., Barnett, R. L., Batterson, M., Bernatchez, P., Borns, H. W., Breckenridge, A., Briner, J. P., Brouard, E., Campbell, J. E., Carlson, A. E., Clague, J. J., Curry, B. B., Daigneault, R.-A., Dubé-Loubert, H., Easterbrook, D. J., Franz, D. A., Friedrich, H. G., Funder, S., Gauthier, M. S., Gowan, A. S., Harris, K. L., Héту, B., Hooyer, T. S., Jennings, C. E., Johnson, M. D., Kehew, A. E., Kelley, S. E., Kerr, D., King, E. L., Kjeldsen, K. K.,
- 575 Knaeble, A. R., Lajeunesse, P., Lakeman, T. R., Lamothe, M., Larson, P., Lavoie, M., Loope, H. M., Lowell, T. V., Lusardi, B. A., Manz, L., McMartin, I., Nixon, F. C., Occhietti, S., Parkhill, M. A., Piper, D. J. W., Pronk, A. G., Richard, P. J. H., Ridge, J. C., Ross, M., Roy, M., Seaman, A., Shaw, J., Stea, R. R., Teller, J. T., Thompson, W. B., Thorleifson, L. H., Utting, D. J., Veillette, J. J., Ward, B. C., Weddle, T. K., and Wright, H. E.: An updated radiocarbon-based ice margin chronology for the last deglaciation of the North American Ice Sheet Complex, *Quaternary Science Reviews*, 234, 106223, <https://doi.org/10.1016/j.quascirev.2020.106223>, 2020.
- 580 Davis, W. R., Collins, M. A., Rooney, T. O., Brown, E. L., Stein, C. A., Stein, S., and Moucha, R.: Geochemical, petrographic, and stratigraphic analyses of the Portage Lake Volcanics of the Keweenaw CFBP: implications for the evolution of main stage volcanism in continental flood basalt provinces, *SP*, 518, 67–100, <https://doi.org/10.1144/SP518-2020-221>, 2022.
- 585 Dell, C. I.: A special mechanism for varve formation in a glacial lake, *Journal of Sedimentary Research*, 43, 838–840, 1973.
- Dell, C. I.: Sediment Distribution and Bottom Topography of Southeastern Lake Superior, *Journal of Great Lakes Research*, 2, 164–176, [https://doi.org/10.1016/S0380-1330\(76\)72283-4](https://doi.org/10.1016/S0380-1330(76)72283-4), 1976.
- Drexler, C. W., Farrand, W. R., and Hughes, J. D.: Correlation of glacial lakes in the Superior basin with eastward discharge events from Lake Agassiz, in: *Glacial Lake Agassiz*, vol. 26, Geological Association of Canada, 309–329, 1983.
- 590 Drexler, C. W.: Outlet Channels for the Post-Duluth Lakes in the Upper Peninsula of Michigan, Ph.D., University of Michigan, Ann Arbor, MI, 407 pp., 1981.

- 595 Dyke, A. S.: An outline of North American deglaciation with emphasis on central and northern Canada, in: *Developments in Quaternary Sciences*, vol. 2, Elsevier, 373–424, [https://doi.org/10.1016/S1571-0866\(04\)80209-4](https://doi.org/10.1016/S1571-0866(04)80209-4), 2004.
- Ehlers, J., Gibbard, P. L., and Hughes, P. D. (Eds.): *Quaternary glaciations - extent and chronology: a closer look*, Elsevier, Amsterdam ; Boston, 1108 pp., 2011.
- Elling, R., Stein, S., Stein, C., and Gefeke, K.: Three Major Failed Rifts in Central North America: Similarities and Differences, *GSAT*, 32, 4–11, <https://doi.org/10.1130/GSATG518A.1>, 2022.
- Farrand, W. R. and Drexler, C. W.: Late Wisconsinan and Holocene history of the Lake Superior basin, *Quaternary Evolution of the Great Lakes*, 30, 17–32, 1985.
- 600 Farrand, W. R.: The Quaternary history of Lake Superior, in: *Proceedings of the 12th Conference of Great Lakes Research*, 181–197, 1969.
- Fisher, T. G. and Breckenridge, A.: Relative lake level reconstructions for glacial Lake Agassiz spanning the Herman to Campbell levels, *Quaternary Science Reviews*, 294, 107760, <https://doi.org/10.1016/j.quascirev.2022.107760>.
- 605 Fisher, T. G. and Whitman, R. L.: Deglacial and Lake Level Fluctuation History Recorded in Cores, Beaver Lake, Upper Peninsula, Michigan, *Journal of Great Lakes Research*, 25, 263–274, [https://doi.org/10.1016/S0380-1330\(99\)70735-5](https://doi.org/10.1016/S0380-1330(99)70735-5), 1999.
- Fisher, T. G., Dziekan, M. R., McDonald, J., Lepper, K., Loope, H. M., McCarthy, F. M. G., and Curry, B. B.: Minimum limiting deglacial ages for the out-of-phase Saginaw Lobe of the Laurentide Ice Sheet using optically stimulated luminescence (OSL) and radiocarbon methods, *Quat. res.*, 97, 71–87, <https://doi.org/10.1017/qua.2020.12>, 2020.
- 610 Fisher, T. G.: Megaflooding associated with glacial Lake Agassiz, *Earth-Science Reviews*, 201, 102974, <https://doi.org/10.1016/j.earscirev.2019.102974>, 2020.
- Flakne, R.: The Holocene vegetation history of Isle Royale National Park, Michigan, U.S.A., *Can. J. For. Res.*, 33, 1144–1166, <https://doi.org/10.1139/x03-063>, 2003.
- Gosse, J. C. and Phillips, F. M.: Terrestrial in situ cosmogenic nuclides: theory and application, *Quaternary Science Reviews*, 20, 1475–1560, [https://doi.org/10.1016/S0277-3791\(00\)00171-2](https://doi.org/10.1016/S0277-3791(00)00171-2), 2001.
- 615 Halfman, J. D. and Johnson, T. C.: Enhanced Atmospheric Circulation over North America During the Early Holocene: Evidence from Lake Superior, *Science*, 224, 61–63, <https://doi.org/10.1126/science.224.4644.61>, 1984.
- Hanson, B. and Hooke, R. LeB.: Glacier calving: a numerical model of forces in the calving-speed/water-depth relation, *J. Glaciol.*, 46, 188–196, <https://doi.org/10.3189/172756500781832792>, 2000.
- 620 Hobbs, H. C. and Breckenridge, A.: Ice advances and retreats, inlets and outlets, sediments and strandlines of the western Lake Superior basin, in: *Archean to Anthropocene: Field Guides to the Geology of the Mid-Continent of North America*, Geological Society of America, 299–315, [https://doi.org/10.1130/2011.0024\(14\)](https://doi.org/10.1130/2011.0024(14)), 2011.
- Huber, N. K.: *Glacial and post glacial geological history of Isle Royale National Park, Michigan*, 1973.
- 625 Hughes, J. D.: *Physiography of a six quadrangle area in the Keweenaw Peninsula north of Portage Lake*, Ph.D., Northwestern University, Evanston, IL, 255 pp., 1963.
- Hyodo, A. and Longstaffe, F. J.: The chronostratigraphy of Holocene sediments from four Lake Superior sub-basins, *Can. J. Earth Sci.*, 48, 1581–1599, <https://doi.org/10.1139/e11-060>, 2011.
- IAGLR: *Large Lakes of the World*, 2012.
- 630 Johnson, T. C. and Fields, J.: Paleomagnetic dating of postglacial sediment, offshore Lake Superior, Minnesota—Wisconsin, U.S.A., *Chemical Geology*, 44, 253–265, [https://doi.org/10.1016/0009-2541\(84\)90076-7](https://doi.org/10.1016/0009-2541(84)90076-7), 1984.
- Johnson, T. C.: Late-Glacial and Postglacial Sedimentation in Lake Superior Based on Seismic-Reflection Profiles, *Quat. res.*, 13, 380–391, [https://doi.org/10.1016/0033-5894\(80\)90064-2](https://doi.org/10.1016/0033-5894(80)90064-2), 1980.
- Jones, R. S., Small, D., Cahill, N., Bentley, M. J., and Whitehouse, P. L.: iceTEA: Tools for plotting and analysing cosmogenic-nuclide surface-exposure data from former ice margins, *Quaternary Geochronology*, 51, 72–86, <https://doi.org/10.1016/j.quageo.2019.01.001>, 2019.
- 635 Kelly, M. A., Fisher, T. G., Lowell, T. V., Barnett, P. J., and Schwartz, R.: <sup>10</sup>Be ages of flood deposits west of Lake Nipigon, Ontario: evidence for eastward meltwater drainage during the early Holocene Epoch, *Can. J. Earth Sci.*, 53, 321–330, <https://doi.org/10.1139/cjes-2015-0135>, 2016.
- 640 Kemp, A. L. W., Dell, C. I., and Harper, N. S.: Sedimentation Rates and a Sediment Budget for Lake Superior, *Journal of Great Lakes Research*, 4, 276–287, [https://doi.org/10.1016/S0380-1330\(78\)72198-2](https://doi.org/10.1016/S0380-1330(78)72198-2), 1978.



- Lal, D.: Cosmic ray labeling of erosion surfaces: in situ nuclide production rates and erosion models, *Earth and Planetary Science Letters*, 104, 424–439, [https://doi.org/10.1016/0012-821X\(91\)90220-C](https://doi.org/10.1016/0012-821X(91)90220-C), 1991.
- Landmesser, C. W., Johnson, T. C., and Wold, R. J.: Seismic Reflection Study of Recessional Moraines beneath Lake Superior and Their Relationship to Regional Deglaciation, *Quat. res.*, 17, 173–190, [https://doi.org/10.1016/0033-5894\(82\)90057-6](https://doi.org/10.1016/0033-5894(82)90057-6), 1982.
- 645 Leydet, D. J., Carlson, A. E., Teller, J. T., Breckenridge, A., Barth, A. M., Ullman, D. J., Sinclair, G., Milne, G. A., Cuzzone, J. K., and Caffee, M. W.: Opening of glacial Lake Agassiz's eastern outlets by the start of the Younger Dryas cold period, *Geology*, 46, 155–158, <https://doi.org/10.1130/G39501.1>, 2018.
- 650 Li, Y.: Determining topographic shielding from digital elevation models for cosmogenic nuclide analysis: a GIS model for discrete sample sites, *J. Mt. Sci.*, 15, 939–947, <https://doi.org/10.1007/s11629-018-4895-4>, 2018.
- Lifton, N., Sato, T., and Dunai, T. J.: Scaling in situ cosmogenic nuclide production rates using analytical approximations to atmospheric cosmic-ray fluxes, *Earth and Planetary Science Letters*, 386, 149–160, <https://doi.org/10.1016/j.epsl.2013.10.052>, 2014.
- 655 Loope, H.: Deglacial chronology and glacial stratigraphy of the western Thunder Bay lowland, northwest Ontario, Canada, M.S., University of Toledo, Toledo, OH, 91 pp., 2006.
- Lowell, T. V., Fisher, T. G., Hajdas, I., Glover, K., Loope, H., and Henry, T.: Radiocarbon deglaciation chronology of the Thunder Bay, Ontario area and implications for ice sheet retreat patterns, *Quaternary Science Reviews*, 28, 1597–1607, <https://doi.org/10.1016/j.quascirev.2009.02.025>, 2009.
- 660 Lowell, T. V., Kelly, M. A., Howley, J. A., Fisher, T. G., Barnett, P. J., Schwart, R., Zimmerman, S. R. H., Norris, N., and Malone, A. G. O.: Near-constant retreat rate of a terrestrial margin of the Laurentide Ice Sheet during the last deglaciation, *Geology*, 49, 1511–1515, <https://doi.org/10.1130/G49081.1>, 2021.
- Lowell, T. V., Larson, G. J., Hughes, J. D., and Denton, G. H.: Age verification of the Lake Gribben forest bed and the Younger Dryas Advance of the Laurentide Ice Sheet, *Can. J. Earth Sci.*, 36, 383–393, <https://doi.org/10.1139/e98-095>, 1999.
- 665 Lowell, T., Waterson, N., Fisher, T., Loope, H., Glover, K., Comer, G., Hajdas, I., Denton, G., Schaefer, J., Rinterknecht, V., Broecker, W., and Teller, J.: Testing the Lake Agassiz meltwater trigger for the Younger Dryas, *Eos Trans. AGU*, 86, 365, <https://doi.org/10.1029/2005EO400001>, 2005.
- Maher, L. J.: Palynological Studies in the Western Arm of Lake Superior, *Quat. res.*, 7, 14–44, [https://doi.org/10.1016/0033-5894\(77\)90012-6](https://doi.org/10.1016/0033-5894(77)90012-6), 1977.
- 670 Marrero, S. M., Phillips, F. M., Borchers, B., Lifton, N., Aumer, R., and Balco, G.: Cosmogenic nuclide systematics and the CRONUScal program, *Quaternary Geochronology*, 31, 160–187, <https://doi.org/10.1016/j.quageo.2015.09.005>, 2016.
- Marshall, S. J., Tarasov, L., Clarke, G. K. C., and Peltier, W. R.: Glaciological reconstruction of the Laurentide Ice Sheet: physical processes and modelling challenges, *Can. J. Earth Sci.*, 37, 769–793, <https://doi.org/10.1139/e99-113>, 2000.
- 675 Mothersill, J. S. and Fung, P. C.: The Stratigraphy, Mineralogy, and Trace Element Concentrations of the Quaternary Sediments of the Northern Lake Superior Basin, *Can. J. Earth Sci.*, 9, 1735–1755, <https://doi.org/10.1139/e72-153>, 1972.
- Mothersill, J. S.: Batchawana Bay, Lake Superior: late Quaternary sedimentary fill and paleomagnetic record, *Can. J. Earth Sci.*, 22, 39–52, <https://doi.org/10.1139/e85-004>, 1985.
- 680 Mothersill, J. S.: Paleomagnetic dating of late glacial and postglacial sediments in Lake Superior, *Can. J. Earth Sci.*, 25, 1791–1799, <https://doi.org/10.1139/e88-169>, 1988.
- Mothersill, J. S.: The paleomagnetic record of the late Quaternary sediments of Thunder Bay, *Can. J. Earth Sci.*, 16, 1016–1023, <https://doi.org/10.1139/e79-089>, 1979.
- 685 Nishiizumi, K., Imamura, M., Caffee, M. W., Southon, J. R., Finkel, R. C., and McAninch, J.: Absolute calibration of  $^{10}\text{Be}$  AMS standards, *Nuclear Instruments and Methods in Physics Research Section B: Beam Interactions with Materials and Atoms*, 258, 403–413, <https://doi.org/10.1016/j.nimb.2007.01.297>, 2007.
- Nishiizumi, K., Winterer, E. L., Kohl, C. P., Klein, J., Middleton, R., Lal, D., and Arnold, J. R.: Cosmic ray production rates of  $^{10}\text{Be}$  and  $^{26}\text{Al}$  in quartz from glacially polished rocks, *J. Geophys. Res.*, 94, 17907, <https://doi.org/10.1029/JB094iB12p17907>, 1989.
- 690 NOAA Great Lakes Environmental Research Lab: Bathymetry of Lake Superior, NOAA National Centers for Environmental Information [data set], <https://www.ncei.noaa.gov/products/great-lakes-bathymetry>, 1999.

- O'Beirne, M. D.: Anthropogenic climate change has driven Lake Superior productivity beyond the range of Holocene variability, Ph.D., University of Minnesota, 142 pp., 2013.
- Paterson, W. S. B.: Laurentide Ice Sheet: Estimated volumes during Late Wisconsin, *Rev. Geophys.*, 10, 885, <https://doi.org/10.1029/RG010i004p00885>, 1972.
- 695 Peltier, W. R., Argus, D. F., and Drummond, R.: Space geodesy constrains ice age terminal deglaciation: The global ICE-6G\_C (VM5a) model: Global Glacial Isostatic Adjustment, *J. Geophys. Res. Solid Earth*, 120, 450–487, <https://doi.org/10.1002/2014JB011176>, 2015.
- Peterson, R. O.: Wolf ecology and prey relationships on Isle Royale, National Park Service, U.S. Department of the Interior, 1977.
- 700 Peterson, W. L.: Surficial geologic map of the Iron River 1 degree by 2 degrees Quadrangle, Michigan and Wisconsin, U.S. Geological Survey, <https://doi.org/10.3133/i1360C>, 1985.
- Raymond, R. E., Kapp, R. O., and Janke, R. A.: Postglacial and recent sediments of inland lakes of Isle Royale National Park, Michigan, *Michigan Academician*, 7, 453–465, 1975.
- Rinterknecht, V. R., Clark, P. U., Raisbeck, G. M., Yiou, F., Bitinas, A., Brook, E. J., Marks, L., Zelčs, V., Lunkka, J.-P., Pavlovskaya, I. E., Piotrowski, J. A., and Raukas, A.: The last deglaciation of the southeastern sector of the Scandinavian Ice Sheet, *Science*, 311, 1449–1452, <https://doi.org/10.1126/science.1120702>, 2006
- 705 Saarnisto, M.: The Deglaciation History of the Lake Superior Region and its Climatic Implications, *Quat. res.*, 4, 316–339, [https://doi.org/10.1016/0033-5894\(74\)90019-2](https://doi.org/10.1016/0033-5894(74)90019-2), 1974.
- Schaetzl, R. J., Lepper, K., Thomas, S. E., Grove, L., Treiber, E., Farmer, A., Fillmore, A., Lee, J., Dickerson, B., and Alme, K.: Kame deltas provide evidence for a new glacial lake and suggest early glacial retreat from central Lower Michigan, USA, *Geomorphology*, 280, 167–178, <https://doi.org/10.1016/j.geomorph.2016.11.013>, 2017.
- Stokes, C. R., Margold, M., Clark, C. D., and Tarasov, L.: Ice stream activity scaled to ice sheet volume during Laurentide Ice Sheet deglaciation, *Nature*, 530, 322–326, <https://doi.org/10.1038/nature16947>, 2016.
- Stone, J. O.: Air pressure and cosmogenic isotope production, *J. Geophys. Res.*, 105, 23753–23759, <https://doi.org/10.1029/2000JB900181>, 2000.
- 715 Stuiver, M. and Reimer, P. J.: Extended 14 C Data Base and Revised CALIB 3.0 14 C Age Calibration Program, *Radiocarbon*, 35, 215–230, <https://doi.org/10.1017/S0033822200013904>, 1993.
- Tarasov, L., Dyke, A. S., Neal, R. M., and Peltier, W. R.: A data-calibrated distribution of deglacial chronologies for the North American ice complex from glaciological modeling, *Earth and Planetary Science Letters*, 315–316, 30–40, <https://doi.org/10.1016/j.epsl.2011.09.010>, 2012.
- 720 Teller, J. T. and Mahnic, P.: History of sedimentation in the northwestern Lake Superior basin and its relation to Lake Agassiz overflow, *Can. J. Earth Sci.*, 25, 1660–1673, <https://doi.org/10.1139/e88-157>, 1988.
- Teller, J. T. and Thorleifson, L. H.: The Lake Agassiz-Lake Superior connection, *Geological Association of Canada Special Paper*, 26, 261–290, 1983.
- 725 Teller, J. T., Boyd, M., Yang, Z., Kor, P. S. G., and Mokhtari Fard, A.: Alternative routing of Lake Agassiz overflow during the Younger Dryas: new dates, paleotopography, and a re-evaluation, *Quaternary Science Reviews*, 24, 1890–1905, <https://doi.org/10.1016/j.quascirev.2005.01.008>, 2005.
- Teller, J. T., Thorleifson, L. H., Dredge, L. A., Hobbs, H. C., and Schreiner, B. T.: Maximum extent and major features of Lake Agassiz, *Geological Association of Canada Special Paper*, 26, 43–45, 1983.
- 730 Teller, J. T., Leverington, D. W., and Mann, J. D.: Freshwater outbursts to the oceans from glacial Lake Agassiz and their role in climate change during the last deglaciation, *Quaternary Science Reviews*, 21, 879–887, [https://doi.org/10.1016/S0277-3791\(01\)00145-7](https://doi.org/10.1016/S0277-3791(01)00145-7), 2002.
- Teller, J. T.: Volume and Routing of Late-Glacial Runoff from the Southern Laurentide Ice Sheet, *Quat. res.*, 34, 12–23, [https://doi.org/10.1016/0033-5894\(90\)90069-W](https://doi.org/10.1016/0033-5894(90)90069-W), 1990.
- 735 Thomas, R. L. and Dell, C. I.: Sediments of Lake Superior, *Journal of Great Lakes Research*, 4, 264–275, [https://doi.org/10.1016/S0380-1330\(78\)72197-0](https://doi.org/10.1016/S0380-1330(78)72197-0), 1978.
- Ullman, D. J., Carlson, A. E., LeGrande, A. N., Anslow, F. S., Moore, A. K., Caffee, M., Syverson, K. M., and Licciardi, J. M.: Southern Laurentide ice-sheet retreat synchronous with rising boreal summer insolation, *Geology*, 43, 23–26, <https://doi.org/10.1130/G36179.1>, 2015.

740 Yu, S.-Y., Colman, S. M., Lowell, T. V., Milne, G. A., Fisher, T. G., Breckenridge, A., Boyd, M., and Teller, J. T.:  
Freshwater Outburst from Lake Superior as a Trigger for the Cold Event 9300 Years Ago, *Science*, 328, 1262–1266,  
<https://doi.org/10.1126/science.1187860>, 2010.